



# Two-stage regional rare-element pegmatite formation at Tysfjord, Norway: implications for the timing of late Svecofennian and late Caledonian high-temperature events

Axel Müller<sup>1,2</sup> · Rolf L. Romer<sup>3</sup> · Lars Eivind Augland<sup>4</sup> · Haoyang Zhou<sup>1</sup> · Nanna Rosing-Schow<sup>1</sup> · John Spratt<sup>2</sup> · Tomas Husdal<sup>1</sup>

Received: 20 September 2021 / Accepted: 22 January 2022 / Published online: 16 February 2022  
© The Author(s) 2022

## Abstract

Pegmatite fields within granite plutons are commonly considered to have formed from residual melts of their host. This is not always true as demonstrated by the Tysfjord granite gneiss and its two groups of pegmatites. The Tysfjord granite gneiss, exposed in a tectonic window of the Caledonides of northern Norway, is part of the transscandinavian igneous belt (TIB) that includes several phases of granitic magmatism. In the northern Hamarøy area (Drag-Finnøy), where most rare-element pegmatites occur, Paleoproterozoic and metamorphosed Group 1 allanite–(Ce)–fluorite metapegmatites have similar bulk rock chemical composition as the TIB granite gneiss rocks, indicating that these pegmatites are residual melts. Group 1 metapegmatites, which are up to 400 m in size, are among the largest known intra-plutonic pegmatites with Nb–Y–F (NYF) signature. The formation of these unusually large granite-hosted NYF pegmatites may have been facilitated by the overall high F content of TIB granite gneisses. Undeformed Group 2 amazonite–tourmaline pegmatites yield columbite and zircon U–Pb ages in the range 400–379 Ma. These pegmatites are interpreted to be anatectic melts that formed from the partial melting of Tysfjord granite gneiss. Group 2 pegmatites, including those from Træna Island and the Sjona tectonic window (400 and 414 Ma), formed during late Caledonian ductile shearing and incipient unroofing of the central Scandinavian Caledonides and record progressively younger ages of this event from SW to NE.

**Keywords** U–Pb dating · Pegmatite · Anatexis · Svecofennian · Caledonian · Tysfjord

## Introduction

Granites in orogenic and anorogenic settings are often spatially associated with pegmatites that may be enriched in incompatible elements. Based on this spatial relation, pegmatites are commonly interpreted to have formed from

residual melts derived from crystallizing granitic plutons (e.g. Černý 1991; Černý and Ercit 2005; London 2008). Such a genetic relation certainly applies for numerous pegmatite fields, in particular for pegmatite fields that are hosted within the parental pluton (e.g. Janeczek 2007; Thomas and Davidson 2016; Falster et al. 2018; Roda-Robles et al. 2018) and that show the same chemical character and age as the associated granite (e.g. Garate-Olave et al. 2017). There is, however, an increasing number of case studies yielding contrasting ages for pegmatites and spatially associated granites and, thus, showing that there are rare-element pegmatites without an associated source granite (e.g. Romer and Smeds 1994, 1996; Fuchsloch et al. 2018; Konzett et al. 2018; Müller et al. 2015, 2017; Schuster et al. 2017; Barros and Menuge 2016; Ilickovic et al. 2017; Knoll et al. 2018; Simmons et al. 1996, 2016; Webber et al. 2019; Fei et al. 2020). These studies imply that not all chemically evolved pegmatites form from residual melts of chemically evolved plutons. The absence of an exposed coeval granite, however,

✉ Axel Müller  
a.b.muller@nhm.uio.no

<sup>1</sup> Natural History Museum, University of Oslo, Blindern, P.O. Box 1172, 0318 Oslo, Norway

<sup>2</sup> Natural History Museum, Cromwell Road, London SW7 5BD, England

<sup>3</sup> GFZ German Research Centre for Geosciences, Telegrafenberg, 14473 Potsdam, Germany

<sup>4</sup> Centre for Earth Evolution and Dynamics (CEED), University of Oslo, Blindern, P.O. Box 1028, 0315 Oslo, Norway

does not exclude the possibility that there is a hidden granite intrusion at depth.

The Paleoproterozoic granites of the Tysfjord–Hamarøy area in north Norway host a suite of pegmatites that traditionally have been interpreted as a typical example of pegmatites being fractionated derivatives of their granitic host. These Paleoproterozoic rocks were metamorphosed and deformed under amphibolite-facies conditions during the Caledonian orogeny about 430 Ma ago (Björklund 1989; Northrup 1997). Based on field observations, there are two generations of pegmatites emplaced in the Paleoproterozoic Tysfjord granite gneiss (Husdal 2008). Although both pegmatite generations show similar mineralogy, the older generation of pegmatites is strongly deformed (sheared and recrystallized and referred to as metapegmatites in the following), whereas the younger generation does not show particular signs of deformation and metamorphic overprint. There are no age data available for these pegmatites, except for a recent study from Hetherington et al. (2021) reporting ages of 400–410 Ma for one of the strongly deformed metapegmatites. A systematically geochronological study is required to explore the possibility that there might be two pegmatite-forming events.

Dating pegmatitic minerals has been challenging as most geochronometers in pegmatites are extremely rich in U and thus have become metamict. Columbite has been proven to be a robust geochronometer as metamict domains preferentially dissolve and thus can be removed. In this study, we present columbite and zircon U–Pb age data for two petrographically and texturally distinct groups of pegmatites within the Tysfjord granite gneiss. We demonstrate that the two groups of pegmatites have different ages, i.e., Paleoproterozoic and Paleozoic, respectively, and are related to late Svecofennian and late Caledonian orogenic processes. We discuss the origin of the two pegmatite generations and their genetic relations with the granitic rocks of the Tysfjord area and the processes that led to the formation of two generations of mineralogically similar rare element pegmatite in the same region.

## Geology of Tysfjord–Hamarøy area

### The Transscandinavian Igneous Belt as part of the Baltic Shield

The Baltic Shield includes an Archean Domain in the north-east, an early Paleoproterozoic Domain, i.e., the Svecofennian Domain, in the central part, and a Neoproterozoic segment, i.e., the Sveconorwegian Domain, in the south-west. Between the Svecofennian and the Sveconorwegian domains lies a major magmatic belt, the Transscandinavian Igneous Belt (TIB, inset in Fig. 1). At the western margin

of the Baltic Shield, all four domains were overprinted by the Caledonian orogen. The Archean domain is dominated by greenstones and trondhjemite–tonalite–granite intrusions. The Svecofennian Domain includes several c. 1.9 Ga magmatic arcs that were accreted to the Archean craton before 1.82 Ga. The boundary between the Archean craton and the various magmatic arcs locally developed into major strike-slip shear zones (inset in Fig. 1). To the south and west, the Svecofennian Domain is succeeded by the 1.85–1.65 Ga TIB (e.g. Gorbatshev 1985; Högdahl et al. 2004). The TIB represent the remains of a former Andean-type magmatic arc, which comprises a giant elongated array of batholiths extending for c. 1400 km from southeasternmost Sweden to Troms in north-western Norway. The magmatic rocks of the TIB belt are not coeval along the belt, which is segmented by the NW–SE striking Paleoproterozoic shear zones extending into the Svecofennian Domain. Within the Caledonian orogen, TIB rocks are exposed in several basement windows. The position of the N–S aligned basement windows is controlled by the former continental margin and the repeatedly reactivated NW–SE striking shear zones (Romer and Bax 1992).

The Tysfjord granite gneiss, which hosts the studied pegmatites, belongs regionally to the TIB. The TIB granites are subalkaline to alkaline, meta- to peraluminous and comprise monzonitic, syenitic and peralkaline granitic plutons, locally with volcanic complexes (e.g., Högdahl et al. 2004). Mafic rocks are abundant in many areas, and mingling/mixing structures are common. Isotopic data show that the TIB has dominantly formed by reworking juvenile (2.1–1.87 Ga) Svecofennian crust, supplemented by mantle material in a continental-arc setting. There are at least two groups of TIB rocks that differ in age and chemical composition. The oldest TIB rocks (TIB-1; 1.85–1.76 Ga) are coeval with post-kinematic granites within the Svecofennian Domain and tend to occur in vicinity of the margin to the domain (Högdahl et al. 2004). The youngest TIB rocks (TIB-2; 1.72–1.65 Ga) dominate the central TIB and partially overlap in age with the rapakivi magmatism in south Finland (e.g. Suominen 1991; Vaasjoki et al. 1991).

### Tectonic development of the Caledonides

The Caledonian orogen is the result of the collision of the continents Laurentia and Baltica in the Silurian, which marks the final stage of the closure of the Iapetus Ocean that had started already in the Ordovician (e.g. Gee and Sturt 1985; Kroner et al. 2020). The nappe complexes of the Scandinavian Caledonides have traditionally been divided into four major tectonic units, named Lower Allochthon, Middle Allochthon, Upper Allochthon, and Uppermost Allochthon, of contrasting provenance and tectonic and metamorphic history (Gee and Sturt 1985; Roberts and Gee 1985; Gee et al.

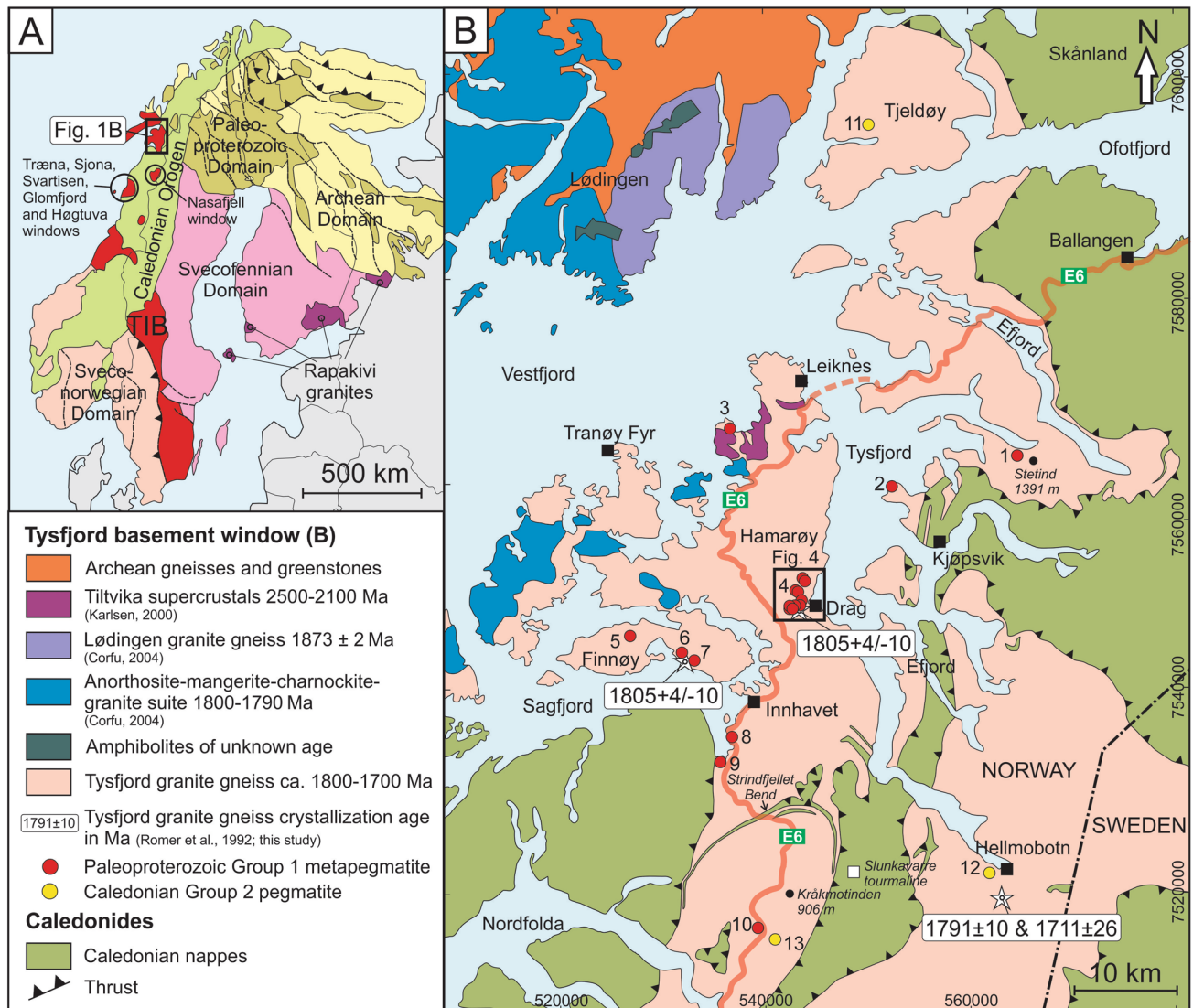


**Fig. 1** A Major Archean and Proterozoic orogens and domains building up Fennoscandia with the location of the study area. Simplified from Bergh et al. (2014). TIB, Transscandinavian Igneous Belt; B simplified geological map of the northern Tysfjord basement window with locations of (meta-)pegmatites of the Tysfjord field. Pegmatites:

Group 1: 1, Stetind; 2, Hundholmen; 3, Tiltvika; 4, Drag metapegmatite cluster including Nedre Øyvollen; 5, Håkonhals; 6, Karlsøy; 7, Oteråga; 8, Lagmannsvik; 9, Elveneset; 10, Kråkmo; Group 2: 11, Tjeldøya; 12, Hellmobotn; 13, Tennvatn

2008; see Corfu et al. 2014 for an in-depth discussion of the tectonostratigraphy; Gee and Stephens 2020). The Lower Allochthon and the Middle Allochthon consist mainly of rocks of the former Baltic margin, the Upper Allochthon includes the zone of continent-ocean transition zone with mafic dike complexes, whereas the Uppermost Allochthon consists dominantly of clastic metasedimentary rocks of the Laurentian margin and former magmatic arc complexes, such as the Bindal Batholith (e.g. Roberts et al. 2007). During the collision, the basement of the Baltic Shield was reworked with regionally contrasting intensity. Major anti-formal stacks of basement rocks, which are exposed in two chains along the Caledonian orogeny, document large-scale

thrusting within the basement (Thelander et al. 1980; Greiling et al. 1993; Rice 2001; Rice and Anderson 2016). The northern and southern margins of the eastern basement windows (e.g. Rombak and Nasafjell) correspond to the NW–SE striking faults in the Svecofennian Domain (Romer and Bax 1992). At these margins, numerous N–S striking faults show minor offset of the contact between the basement and its sedimentary cover, providing direct evidence that the basement was reworked during the Caledonian orogeny. In fact, the structure of the Strindfjellet Bend in the central Tysfjord window (Fig. 1B) documents that the Tysfjord granite gneiss was locally thrust over rocks of the Caledonian nappes.

Towards the centre of the basement windows, these numerous small faults combine to larger N–S striking steeply dipping faults with major offset, causing the highest culminations of granitic basement in the centre of the windows to be more than 1300 m higher than the basement-cover contact at the northern and southern margins of the windows (cf. Romer and Bax 1992; Romer et al. 1994). The western basement windows, including the Tysfjord window, experienced a similar reworking during the Caledonian orogeny, although at higher metamorphic grade and with more intense deformation of the granitic rocks. Within these windows, folds, fold-trains, lineations and S–C fabrics preserve a top–ENE transport direction interpreted to record early thrusting and nappe emplacement, probably near the onset of continental collision (Larsen et al. 2002; Osmundsen et al. 2003). The gneissose foliation of the basement rocks is suggested to have evolved during the antiformal stacking and unroofing of the gneissic-granite-cored culminations (Gromet and Andresen 1993; Larsen et al. 2002; Dewey and Strachan 2003; Osmundsen et al. 2003).

The former basement and Caledonian nappes underwent different grades of prograde and retrograde metamorphism ranging from greenschist to high-grade amphibolite facies (c. 430–410 Ma; Northrup 1997; Steltenpohl et al. 2003). Post-orogenic extension (c. 410–380 Ma) was related to the beginning collision between Gondwana and Laurentia in the south (Fossen 2010; Kroner et al. 2020). The widespread, Early–Mid-Devonian top–W to –SW ductile extension resulted in the reactivation of N–S to NW–SE striking faults (Eide et al. 2002).

### The Tysfjord basement window

The Tysfjord pegmatites and granite gneiss are exposed in a tectonic window in the Caledonides of northern Norway, the Tysfjord basement window. The Tysfjord granite gneisses occupy about 4000 km<sup>2</sup> and cover almost the entire window (Fig. 1). Only in the north and north-west, at Hamarøy, volcanic and sedimentary Svecofennian supracrustal rocks with ages of 2500–2100 Ma and 1910–1880 Ma are preserved (Karlsen 2000). To the north of Vestfjorden, the window continues into the Lofoten–Vesterålen basement complex. The oldest rocks of that complex are remnants of an Archean greenstone belt that have been intruded by anorthositic, mangeritic, charnockitic, and granitic (AMCG) rocks (Griffin et al. 1978) between 1870 and 1790 Ma (e.g. Corfu 2004) and by the Tysfjord granite gneiss, which form the Tjeldøya island (Fig. 1). In the west, south and southeast, the Tysfjord window is framed by overlying Caledonian nappe complexes. The nappes belong to the upper part of the

Upper Allochthon and the Uppermost Allochthon. The Upper Allochthon, to the west and south of the Tysfjord window, forms an up to 5 km thick nappe stack comprising the Narvik, Ofoten and Niingen Nappe Complexes (Barker 1986; Steltenpohl and Bartley 1987; Andresen and Steltenpohl 1994; Anderson and Barker 1999). The Uppermost Allochthon in the south consists of the Fauske and Rødingsfjellet Nappe Complexes (e.g. Roberts et al. 2007).

### The Tysfjord granite gneiss

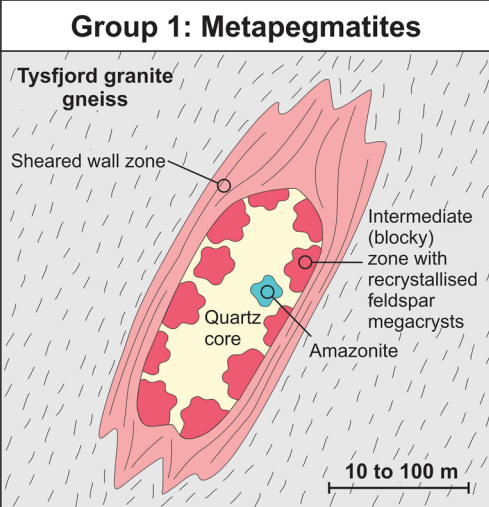
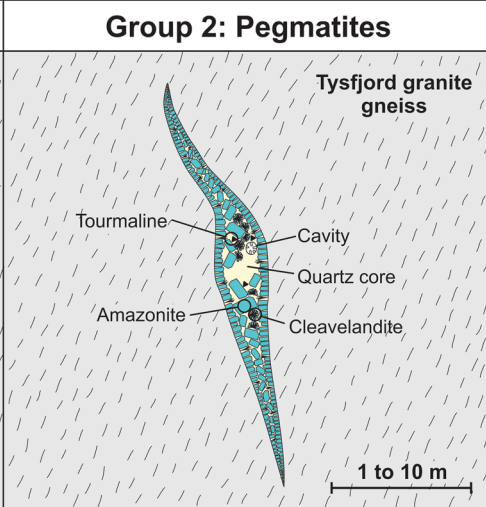
The Tysfjord granite gneiss is a coarse-grained, foliated, pale grey to pale red, partly recrystallized metagranite with biotite, hornblende, quartz, K-feldspar, and oligoclase-albite. Accessory minerals include allanite-(Ce), titanite, zircon, apatite, magnetite, fluorite, polycrase-(Y), and thorianite (Müller 2011). The emplacement of the TIB is related to the last stage of the Svecofennian orogeny (1.92–1.79 Ga; Lahtinen et al. 2008, 2009). The TIB has been interpreted as an Andean-type belt or as a continental belt (Högdahl et al. 2004). The TIB magmatism has been tentatively separated into two different episodes: the little fractionated, TIB-1 group with predominant I-type signature and emplacement ages of 1850 to 1760 Ma and the more fractionated TIB-2 group of A-type affinity with ages between 1720 and 1650 Ma (Skår 2002; Högdahl et al. 2004; Lahtinen et al. 2008). Both groups occur in the Tysfjord window (Romer et al. 1992). Samples from the Hellmobotn (25 km SE of Drag) have a bimodal U–Pb zircon age distribution of  $1791 \pm 10$  Ma (TIB-1) and  $1711 \pm 26$  Ma (TIB-2), respectively (Romer et al. 1992) (Fig. 1). The foliation and recrystallization of the granites extends at least 2500 m down from the overlying (now eroded) Caledonian nappes (Andresen and Tull 1986). The foliation developed under amphibolite-facies conditions during the Caledonian orogeny at c. 432 Ma (Northrup 1997).

### The Tysfjord (meta-)pegmatites

The Tysfjord pegmatites are of the Nb–Y–F (NYF) type (applying the classification of Černý 1991) and occur within the Tysfjord granite gneiss. Major minerals are quartz, K-feldspar, plagioclase and biotite. Main accessory minerals are allanite-(Ce), fergusonite-(Y), columbite-(Fe), thalénite-(Y), gadolinite-(Y), beryl, various sulfides (pyrite, pyrrhotite, arsenopyrite) and Y-rich fluorite with abundant inclusions of various REE-minerals (Husdal 2008).

Pegmatite mining has a more than 100-year long tradition in the Tysfjord–Hamarøy area. Mining of ceramic feldspar started at Hundholmen in 1906 and in numerous pegmatites in the Drag area in 1907, and lasted until the 1970s. Mining took up again in 1996 at Nedre Øyvollen, this time for the



	Group 1: Metapegmatites	Group 2: Pegmatites
Structure		
Size	Large, up to 1.5 million m <sup>3</sup>	Small, <1000 m <sup>3</sup>
Shape	Lenticular to cigar-shaped	Dyke-like
Indicative main minerals	Pink and white K-feldspar (amazonite is very rare), biotite, plagioclase	Amazonite as only K-feldspar, albite (cleavelandite), poor in mica
Indicative accessories	Allanite-(Ce), beryl, fluorite, thalénite-(Y), sulfides	Tourmaline, beryl, fluorite, gadolinite group minerals
Chemistry	Primitive to moderately evolved NYF	Highly evolved NYF
Deformation	Recrystallized and sheared	Undeformed
Other	Pegmatite is massive (no cavities) and concordant to host rock foliation	Pegmatite has small cavities and is discordant to host rock foliation

**Fig. 2** Structural and mineralogical features of Group 1 metapegmatites and Group 2 pegmatites of the Tysfjord basement window

production of high purity quartz (quartz with < 50 ppm contaminating elements). The Nedre Øyvollen and Håkonhals pegmatites, and most of the other Tysfjord pegmatites, contain quartz whose exceptionally low concentrations of trace elements made it applicable to specific high-tech products, such as quartz glass crucibles. Compared with quartz from other pegmatites, the Tysfjord pegmatite quartz is one of the purest worldwide (Müller et al. 2013).

Husdal (2008) distinguished two genetic groups of pegmatites within the Tysfjord field based on their degree of deformation and average body size (Fig. 2). Group 1 metapegmatites underwent ductile deformation resulting in large-scale shearing of the pegmatite bodies and partial or complete recrystallization of pegmatite minerals (Fig. 3A and B). Because of the deformation, the primary magmatic zoning of the metapegmatites—border, wall, intermediate and core zones—is preserved only locally. The fine- to medium-grained granitic wall zone shows a distinct foliation, which is parallel to the metapegmatite contacts. The wall zone gradually changes into large, irregularly shaped masses of recrystallized megacrystic K-feldspar and plagioclase embedded in quartz, representing the intermediate

zone. In this zone, K-feldspar is much more common than plagioclase. Most Group 1 metapegmatites have a massive quartz core (Fig. 2). In the strongly deformed metapegmatites, such as Håkonhals, large-scale (5–20 m) boudins of the intermediate zone and core are blended. Characteristic accessory minerals are allanite-(Ce), fluorite, thalénite-(Y), beryl and sulphides (pyrrhotite, löllingite, galena, pyrite and chalcopyrite). Most Group 1 metapegmatites, 21 bodies, occur around the village Drag, aligned at a 4 km long structure (Fig. 4). Additional Group 1 metapegmatites (about 10 bodies) seem to be randomly distributed across the northern Tysfjord basement window.

Group 2 pegmatites occur as preferentially N–S-striking, dyke-like bodies, which were not affected by deformation (Figs. 2 and 3C). Distinct mineralogical zoning and ‘cleavelandite’ (platy shape variety of albite) replacement zones are developed. Intense green coloured K-feldspar (amazonite) and abundant black tourmaline are typical for Group 2 pegmatites (Fig. 3D). Typical accessory minerals are schorl, magnetite, beryl, fluorite, gadolinite group minerals, helvine group minerals, columbite-(Mn), columbite-(Fe), various Pb–Bi sulfides

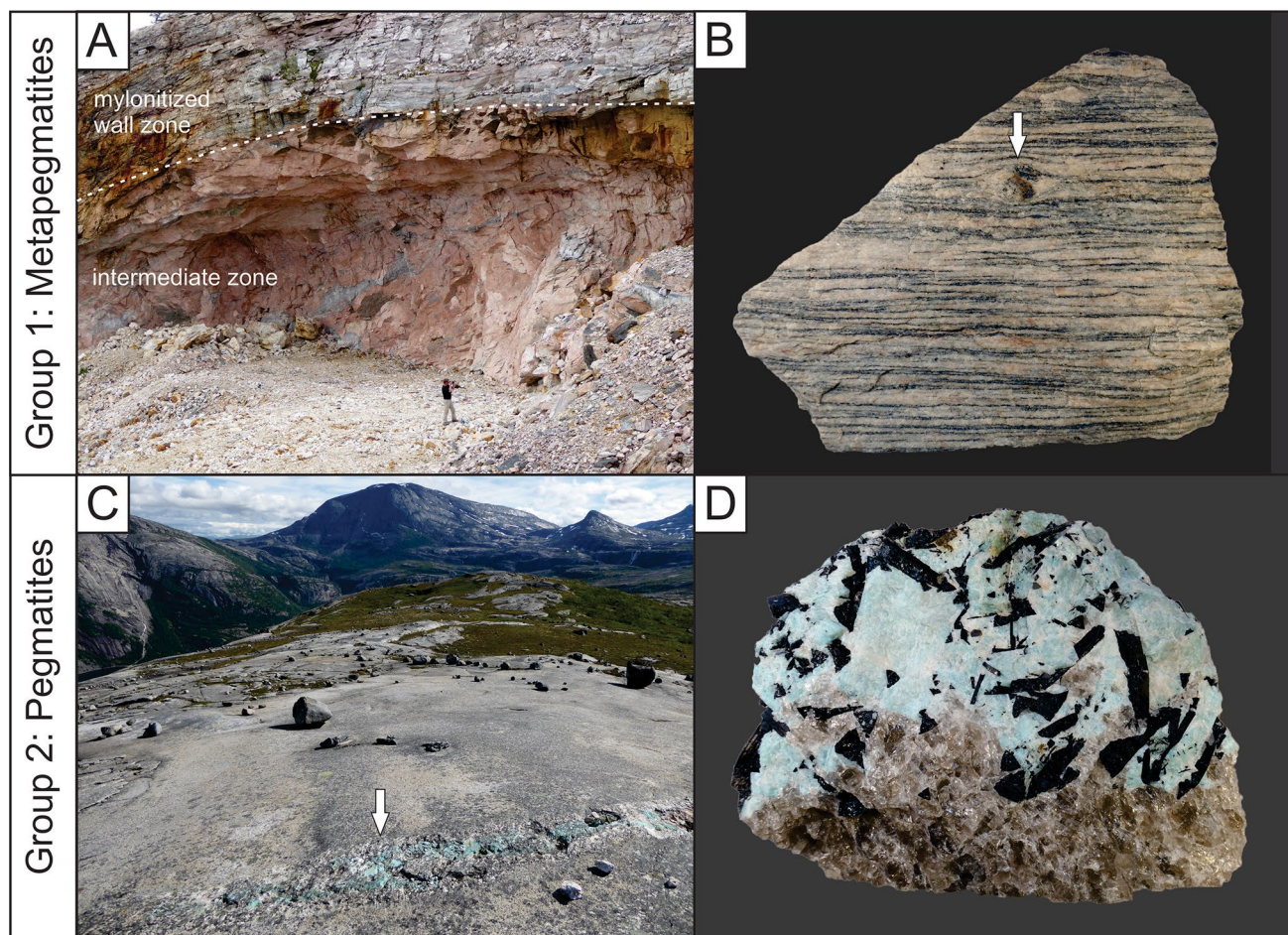


**Fig. 3** **A** North wall of the Håkonhals mine exposing the uppermost part of the Håkonhals Group 1 metapegmatite comprising the up to 8 m thick mylonitized wall zone and the K-feldspar-dominated intermediate zone. See person for scale. **B** Hand specimen (14 cm in length) of the mylonitized wall zone of the Håkonhals metapegma-

tite with an allanite-(Ce) phenoclast (arrow). The dark layers consist of magnetite and biotite. **C** Dyke-like, up to 1 m wide Group 2 amazonite pegmatite at Hellmobotn (arrow). **D** Amazonite-tourmaline-quartz assemblage of the Group 2 Tjeldøya pegmatite

and sulfosalts, zircon, thorite, xenotime-(Y) and metamict (Mn,Fe)-Y-(Sb,As)-(Nb,Ti) oxide. In contrast to most Group 1 metapegmatites, Group 2 pegmatites occur relatively near the edge of the Tysfjord basement window, and, thus, immediately below the now eroded thrust (Fig. 1).

## Methods

### Sampling

For this study, we selected columbite group minerals for U-Pb dating from the mineral collection of the Natural History Museum of Oslo (samples Hundholmen MIN 27459 and Tiltvika MIN 17265). Specimens were also collected from the active Nedre Øyvollen underground mine at Drag and from the Tjeldøya pegmatite (with both columbite and zircon). The columbite sample from the Tennvatn pegmatite

was provided by the mineral collector Astrid Haugen. In addition, two Tysfjord granite gneiss varieties, one next to the Jennyhaugen metapegmatite at Drag and one at Finnøy Island next to the Karlsøy metapegmatite, were sampled for zircon dating and for whole rock analysis.

To estimate the composition of Group 1 metapegmatites, three 5-kg samples were taken from the medium- to coarse-grained wall zone of the Jennyhaugen metapegmatite. The wall zone of pegmatites crystallized first. Therefore, it may better represent the initial composition of the pegmatite melt, although the wall zone may contain lower concentrations of incompatible elements than more evolved zones (e.g., Müller et al. 2021).

### Electron probe microanalysis

The compositions of columbite-group minerals were determined using a Cameca SX100 electron microprobe at the



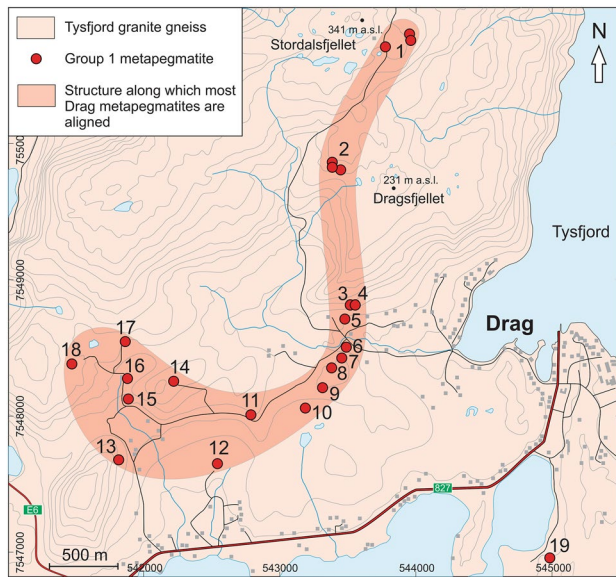


**Fig. 4** Geological map showing the metapegmatite locations in the vicinity of the village Drag. Pegmatite mines (names according to Åmli 1975): 1, Fjellgruvene; 2, Nekkaltelgruvene; 3, Øvre Øyvollen; 4, Perjongruva; 5, Nedre Øyvollen; 6, Grønnhola; 7, Kvartsbrudd Øst; 8, Burma; 9, Jennyhaugen; 10, Sumpa; 11, Lillebakkgruvene; 12, Lillebakkmyra; 13, Bennygruva; 14, Svenskgruva; 15, Nedre Lapplægret; 16, Øvre Lapplægret; 17, Kvartsbrudd Nordre; 18, Vestre Trettbakken; 19, Hammondgruva

Natural History Museum of London. The samples were prepared as surface-polished, one-inch epoxy mounts. Instrument beam conditions were 20 kV and 20 nA with a 1  $\mu$ m spot size. The Cameca supplied PAP matrix correction was used. Peak overlaps were corrected prior to matrix correction for the most severe peak overlaps.

### TIMS U–Pb dating of columbite-group minerals

Columbite-group minerals were dated at GFZ German Research Centre for Geosciences, Potsdam, Germany using the sample preparation procedures described in Romer and Smeds (1996) and Baumgartner et al. (2006). Isotope ratios were determined with a Triton multi-collector mass spectrometer using Faraday collectors and ion counting, operated in static multi-collection mode. The analytical results are shown in (Table 1).

All samples were leached. The rationale behind the leaching and annealing procedures is the following: columbite-group minerals commonly have elevated U contents (a few hundred to several thousand ppm) that may be heterogeneously distributed within the mineral and that with time lead to metamictization beginning in particularly U-rich domains (Romer et al. 2007). Metamict domains may experience significant redistribution of U and Pb, leading on the small scale to overall loss or gain of U and Pb. Locally there

may also be additions of common Pb. To avoid problems related to such open system behaviour of the U–Pb system in columbite-group minerals, selected fragments were leached in 20% HF (20 min at 70 °C), followed by washing steps using 6 N HCl and 7 N HNO<sub>3</sub>, respectively (20 min each at 70 °C). This leaching procedure using different acids typically removes fracture fills and inclusions of quartz, feldspar, sulphides, and metamict domains. The selective dissolution procedure usually results in higher <sup>206</sup>Pb/<sup>204</sup>Pb values (Romer and Wright 1992) as carriers of common Pb (feldspar and sulphide inclusions) are preferentially removed and in favourable cases yields concordant data (Romer and Smeds 1996; Lindroos et al. 1996). The higher common Pb contents in some samples largely are due to the larger size of the fragments of the columbite-group minerals used, essentially reflecting the less efficient removal of damaged sections in larger fragments. Incomplete removal of metamict domains may preferentially mobilize Pb or U and, thus, result in laboratory induced normal or reverse discordance. Incompletely leached columbite-group minerals typically develop a brown stain during the final leaching step, rather than metallic luster (Romer 2003). Some columbite-group minerals from Tysfjord (meta-)pegmatites showed such anomalous leaching behaviour, as repeated leaching did not produce surfaces with metallic luster or dissolved the mineral completely. This behaviour reflects that the mineral is almost completely metamict.

To prevent complete sample dissolution during the sample leaching procedure, two samples were annealed at 650 °C for 60 min before leaching. Annealing prevents complete dissolution of the mineral during the later leaching procedure, but preserves disturbances originating from element mobility in the metamict domains. Thus, annealed samples do not produce precise ages, but tend to produce scattered data about a Discordia. The Discordia intercept ages of annealed samples represent a good estimate for the age, but should not be considered to be accurate.

### TIMS U–Pb dating of zircon

The samples were crushed, ground and passed over a Wilfley table before heavy minerals were separated using standard heavy liquid and magnetic techniques at the University of Oslo (except from the Tjeldøya zircon, see above). Zircons were selected under an optical microscope, annealed for ca. 72 h at ca. 900 °C and chemically abraded with HF in a high-pressure dissolution vessel at ca. 195 °C for 12 h (Huyskens et al. 2016; Mattinson 2005). The zircon grains chosen for analyses were spiked with the <sup>205</sup>Pb–<sup>233</sup>–<sup>235</sup>U EARTH-TIME (ET) tracer (Condon et al. 2015). After spiking, zircon samples were dissolved in HF (+HNO<sub>3</sub>) at > 48 h in Teflon micro capsules enclosed in a Parr type Teflon bomb and the solutions were subsequently passed through column

**Table 1** U–Pb analytical results for columbite from (meta-)pegmatites of the Tysfjord area, northern Norway

Sample <sup>a</sup>	Weight (mg)	Concentrations (ppm)		Common lead (pg)	Radiogenic Pb (at%) <sup>c</sup>			Th/U <sup>d</sup>	Atomic ratios <sup>e</sup>			Apparent ages (Ma) <sup>e</sup>			
		U	Pb		<sup>206</sup> Pb	<sup>207</sup> Pb	<sup>208</sup> Pb		<sup>206</sup> Pb/ <sup>238</sup> U	<sup>207</sup> Pb/ <sup>235</sup> U	<sup>206</sup> Pb/ <sup>207</sup> Pb	<sup>206</sup> Pb/ <sup>238</sup> U	<sup>207</sup> Pb/ <sup>235</sup> U	<sup>206</sup> Pb/ <sup>207</sup> Pb	
Hundholmen, Tysfjord															
Hun-1	0.180	98.5	25.2	1468	89.47	9.34	1.19	0.04	0.25690	3.6985	0.10442	1474	1571	1704	
Hun-2	0.228	78.9	34.1	734	88.39	9.78	1.84	0.07	0.41152	6.2772	0.11063	2222	2015	1810	
Hun-3	0.211	55.1	26.7	390	87.43	9.74	2.83	0.10	0.42770	6.5699	0.11141	2295	2055	1823	
Hun-4	0.127	78	22.3	908	89.49	9.47	1.04	0.04	0.28143	4.1065	0.10583	1599	1656	1729	
Tiltvika, Tysfjord															
Til-1	0.440	81.8	28.3	2058	87.36	9.56	3.05	0.11	0.34952	5.2884	0.10974	1932	1867	1795	
Til-2	0.207	78.3	33.5	1948	86.67	9.70	3.63	0.13	0.41970	6.4784	0.11195	2259	2043	1831	
Til-3	0.287	79.4	24.0	1879	87.64	9.42	2.94	0.11	0.29893	4.4306	0.10750	1686	1718	1757	
Til-4	0.478	33.1	13.6	2010	86.83	9.70	3.47	0.13	0.40356	6.2132	0.11166	2185	2006	1827	
Nedre Øyvollen, Tysfjord															
Dra-1	0.256	673	63.1	675	82.00	6.42	11.58	0.44	0.08254	0.89079	0.07827	511	647	1154	
Dra-2	0.211	373	45.9	758	85.89	7.86	6.25	0.23	0.11406	1.4395	0.09153	696	906	1458	
Dra-3	0.255	625	59.8	185	85.72	6.63	7.65	0.28	0.05905	0.63011	0.07739	370	496	1131	
Dra-4	0.238	615	70.8	147	85.79	5.66	8.55	0.31	0.07967	0.72505	0.06600	494	554	806	
Dra-5	0.197	294	28.2	211	85.70	6.60	7.70	0.28	0.07387	0.78394	0.07697	459	588	1120	
Dra-6	0.139	286	53.1	86	84.24	6.40	9.36	0.35	0.10002	1.0480	0.07600	615	728	1095	
Tennvatn, Tysfjord															
Ten-1	0.513	180	12.3	306	94.74	5.05	0.31	0.01	0.06087	0.4473	0.05329	381	375	341	
Ten-2	0.266	199	11.4	1843	94.26	5.11	0.63	0.02	0.06071	0.4535	0.05417	380	380	377	
Ten-3	0.098	213	12.2	2026	94.25	5.10	0.65	0.02	0.06172	0.4610	0.05416	386	385	377	
Ten-4	0.159	208	18.1	143	93.93	5.04	1.03	0.04	0.06170	0.4567	0.05369	386	382	358	
Ten-5	0.612	212	12.3	1531	94.40	5.08	0.52	0.02	0.06107	0.4532	0.05381	382	380	363	
Tjeldøya, Tysfjord															
Tje-1	0.422	152	9.1	2590	93.52	5.10	1.38	0.05	0.06353	0.4776	0.05453	397	397	393	
Tje-2	0.470	203	11.5	8407	93.81	5.06	1.13	0.04	0.06170	0.4589	0.05395	386	384	369	
Tje-3	0.407	199	13.7	375	93.31	5.07	1.62	0.06	0.06304	0.4722	0.05432	394	393	384	



Table 1 (continued)

Sample <sup>a</sup>	Weight (mg)	Concentrations (ppm)		Common lead (pg)	Radiogenic Pb (at%) <sup>c</sup>			Th/U <sup>d</sup>	Atomic ratios <sup>e</sup>			Apparent ages (Ma) <sup>e</sup>			
		U	Pb		<sup>206</sup> Pb	<sup>207</sup> Pb	<sup>208</sup> Pb		<sup>206</sup> Pb/ <sup>238</sup> U	<sup>207</sup> Pb/ <sup>235</sup> U	<sup>206</sup> Pb	<sup>207</sup> Pb	<sup>238</sup> U	<sup>206</sup> Pb	<sup>207</sup> Pb
Tje-4	0.161	206	12.2	41	93.67	5.12	1.22	0.04	0.06329	0.4768	0.05464	396	396	396	397
Tje-5	0.110	136	8.5	50	93.55	5.11	1.34	0.05	0.06414	0.4827	0.05458	401	400	400	395
Tje-6	0.134	164	9.8	21	93.52	5.10	1.38	0.05	0.06405	0.4810	0.05450	400	399	400	392

<sup>a</sup>Small fragments from single columbite grains. Samples Hundsholmen and Tiltvok were annealed before leaching. All samples were leached before dissolution (for details see text)

<sup>b</sup>Lead isotope ratios corrected for fractionation, blank and isotopic tracer. Samples were analyzed at GFZ German Research Centre for Geosciences, Potsdam, Germany, using a <sup>205</sup>Pb-<sup>235</sup>U mixed isotopic tracer. Analytical details are given in Romer and Smeds (1996) and Baumgartner et al. (2006). During the measurement period total blanks were less than 15 pg for lead and less than 1 pg for uranium

<sup>c</sup>Lead corrected for fractionation, blank, isotopic tracer, and initial lead with the composition according to Stacey and Kramers (1975)

<sup>d</sup><sup>232</sup>Th/<sup>238</sup>U calculated from radiogenic <sup>206</sup>Pb/<sup>206</sup>Pb and the age of the sample

<sup>e</sup>Apparent ages were calculated using the constants of Jaffey et al. (1971) recommended by IUGS.  $\lambda_{238} = 1.55125 \text{ E-10 year}^{-1}$ ,  $\lambda_{235} = 9.848 \text{ E-10 year}^{-1}$

chemistry (separating U and Pb from REE's and other ionisation inhibiting elements). The solutions were loaded on zone refined Re filaments and measured on a Finnigan MAT262 thermal ionisation mass spectrometer (TIMS). The mass spectrometric techniques used are presented in detail in Ballo et al. (2019), with upgraded laboratory parameters: Pb blank generally < 1.2 pg with a composition of <sup>206</sup>Pb/<sup>204</sup>Pb = 18.04 ± 0.40; <sup>207</sup>Pb/<sup>204</sup>Pb = 15.22 ± 0.30; <sup>208</sup>Pb/<sup>204</sup>Pb = 36.67 ± 0.50. The raw data were cleaned using Tripoli (Bowring et al. 2011) and further reduced including calculation of analytical errors and corrections (including Th-corrections, assuming Th/U in the magma of 3) were incorporated and propagated using an Excel macro based on published algorithms (Schmitz and Schoene 2007). Concordia diagrams were generated and intercept ages were calculated using ISOPLOT (Ludwig 2003) with specified decay constants (Jaffey et al. 1971). The ages are reported with ± x/y/z errors, where x only includes the analytical uncertainties, y is the error including the analytical and tracer calibration uncertainties and z is the error including the analytical uncertainties, tracer uncertainties and uncertainty in the decay constant (Table 2).

## Results

### Chemistry of the Tysfjord granite gneiss and Group 1 metapegmatites

Bulk rock analyses were performed on the two Tysfjord granite gneiss samples from Karlsøy and Jennyhaugen, of which zircon was separated for dating. In addition, published whole rock data of other granite localities of the northern Tysfjord window and of one Group 1 metapegmatite wall zone composition are considered in the following (Romer et al. 1992; Müller 2011). The complete data set is provided in the Supplementary Material Table SM1.

Generally, the Tysfjord granite gneiss in the northern Tysfjord window is metaluminous to peraluminous (A/CNK = 0.9–1.1) rocks with low TiO<sub>2</sub> (mean 0.39 wt.%), Sr (mean 92 ppm) and P<sub>2</sub>O<sub>5</sub> (mean 0.08 wt.%) (Fig. 5). The fractionated granites are enriched in K, F, Rb, Th, U, Nb, Y, REE, Hf, and Zr. Fluorine concentrations reach up to 0.45 wt.%. The older TIB-1 granites show little chemical variation, whereas the more fractionated TIB-2 granites, characterised by high 1/TiO<sub>2</sub> ratios (Fig. 5), show variable chemical compositions with enrichment of LREE, Th, U, Nb, Ta, Hf and Zr. The REE patterns show a strong enrichment of LREE relative to HREE and a moderate negative Eu anomaly, which is more pronounced in the TIB-2 than in TIB-1. Due to their elevated REE, Zr and Nb contents (REE + Zr + Nb > 350 ppm), granite samples from Jennyhaugen, Karlsøy, Hundsholmen and Kjerrfjell and most of the

**Table 2** U–Pb analytical results for zircon from granite gneisses and pegmatites of the Tysfjord area, northern Norway

Sample	Composi- tion		Radiogenic isotope ratios								Isotopic ages					
	Th	Pb <sub>c</sub>	<sup>206</sup> Pb		<sup>207</sup> Pb		<sup>206</sup> Pb		Corr Coef	<sup>207</sup> Pb		<sup>207</sup> Pb		<sup>206</sup> Pb		
			<sup>204</sup> Pb	<sup>206</sup> Pb	% err	<sup>235</sup> U	% err	<sup>238</sup> U		% err	<sup>206</sup> Pb	±	<sup>235</sup> U	±	<sup>238</sup> U	±
(a)	(b)	(c)	(d)	(e)	(f)	(e)	(f)	(e)	(f)		(g)	(f)	(g)	(f)	(g)	(f)
2922 Jennyhaugen, Tysfjord granite																
610/1	0.31	2.39	17,742	0.106552	0.043	3.859	0.15	0.26268	0.13	0.962	1741.24	0.79	1605.2	1.2	1503.5	1.8
610/2	0.33	3.30	3056	0.106669	0.065	3.924	0.16	0.26680	0.11	0.950	1743.3	1.2	1618.6	1.3	1524.5	1.5
610/3	0.40	2.06	8798	0.106818	0.094	3.933	0.14	0.267074	0.088	0.726	1745.8	1.7	1620.6	1.1	1525.9	1.2
610/4	0.25	1.05	791	0.107091	0.163	4.077	0.30	0.27614	0.14	0.978	1750.5	3.0	1649.8	2.4	1571.9	2.0
610/5	0.27	1.26	292	0.100375	0.553	2.890	0.68	0.20881	0.17	0.832	1631	10	1379.3	5.2	1222.5	1.9
3122 Karlsøy, Tysfjord granite																
610/6	0.32	1.68	1363	0.101868	0.089	2.905	0.13	0.206859	0.070	0.799	1658.4	1.7	1383.3	1.0	1212.06	0.78
610/7	0.26	2.04	294	0.103281	0.790	3.399	0.96	0.23871	0.185	0.957	1684	15	1504.2	7.6	1380.0	2.3
610/8	0.49	4.93	4454	0.109732	0.047	4.705	0.12	0.310958	0.095	0.934	1794.97	0.86	1768.1	1.0	1745.4	1.5
610/9	0.50	1.63	20,145	0.109192	0.042	4.585	0.14	0.30457	0.119	0.958	1785.98	0.77	1746.6	1.2	1713.9	1.8
610/10	0.42	1.41	7324	0.107983	0.072	4.218	0.21	0.28328	0.185	0.936	1765.7	1.3	1677.5	1.7	1607.9	2.6
Tjeldøya pegmatite																
616/10	0.04	0.86	29,946	0.054594	0.16	0.4729	0.27	0.062817	0.20	0.804	395.6	3.6	393.16	0.87	392.74	0.77

<sup>a</sup>Single zircon fraction chemically abraded (Mattinson, 2005)

<sup>b</sup>Model Th/U ratio iteratively calculated from the radiogenic <sup>208</sup>Pb/<sup>206</sup>Pb ratio and <sup>206</sup>Pb/<sup>238</sup>U age

<sup>c</sup>Pb<sub>c</sub> represents common Pb

<sup>d</sup>Measured ratio corrected for spike and fractionation only. Pb fractionation estimated at 0.16 ± 0.03%/a.m.u. for SEM analyses, based on repeated analysis of NBS982

<sup>e</sup>Corrected for fractionation, spike, and common Pb; up to 2 pg of common Pb was assumed to be procedural blank: <sup>206</sup>Pb/<sup>204</sup>Pb = 18.07 ± 0.30%; <sup>207</sup>Pb/<sup>204</sup>Pb = 15.57 ± 0.20%; <sup>208</sup>Pb/<sup>204</sup>Pb = 37.85 ± 0.30% (all uncertainties 1-sigma). Excess over blank was assigned to initial common Pb, using the Stacey and Kramers (1975) two-stage Pb isotope evolution model at the nominal sample age

<sup>f</sup>Errors are 2-sigma, propagated using the algorithms of Schmitz and Schoene (2007)

<sup>g</sup>Calculations are based on the decay constants of Jaffey et al. (1971). <sup>206</sup>Pb/<sup>238</sup>U and <sup>207</sup>Pb/<sup>206</sup>Pb ages corrected for initial disequilibrium in <sup>230</sup>Th/<sup>238</sup>U using Th/U [magma] = 3

samples from Hellmobotn classify as A-type granites. Some TIB-1 granites and some of the less fractionated TIB-2 granites from Hellmobotn have I-type characteristics.

The average major element composition of the wall zone of the Jennyhaugen metapegmatite resembles that of the most evolved granite gneiss samples (Fig. 5). The major differences between metapegmatite and granite gneisses are the strong depletion in LREE and the pronounced negative Eu anomaly in the metapegmatites.

## Tysfjord granite gneiss U–Pb zircon dating

### Jennyhaugen (sample 2922)

Five single zircon crystals were analysed from Tysfjord granite gneiss exposed next to the Jennyhaugen metapegmatite. All grains were euhedral, prismatic with a medium to high aspect ratio (1:3–1:5) and with relatively abundant inclusions. The zircon crystals display varying degrees of

metamictisation, with some grains having heavily metamict domains. Cathodoluminescence images of zircon crystals show complex zonation with a mixture of sector zoning and oscillatory zoning, indicating recrystallisation during a metamorphic event. All analysed zircon crystals (analyses 610/1–610/5), even those with simple zonation, and a zircon tip with faint sector zonation are discordant (Table 2; Fig. 6). With the exception of the zircon tip (610/5), the zircon analyses project towards an upper intercept age of c. 1772 ± 9 Ma (2σ; MSWD = 2.8). Using only the zircon tip (610/5) and the least discordant zircon prism (610/4), the data yield an upper intercept age of 1801 ± 6 Ma (2σ). The remaining analyses plot below this two-point discordia line, reflecting Pb-loss/recrystallization during a late Caledonian event and Pb-loss from metamict domains.

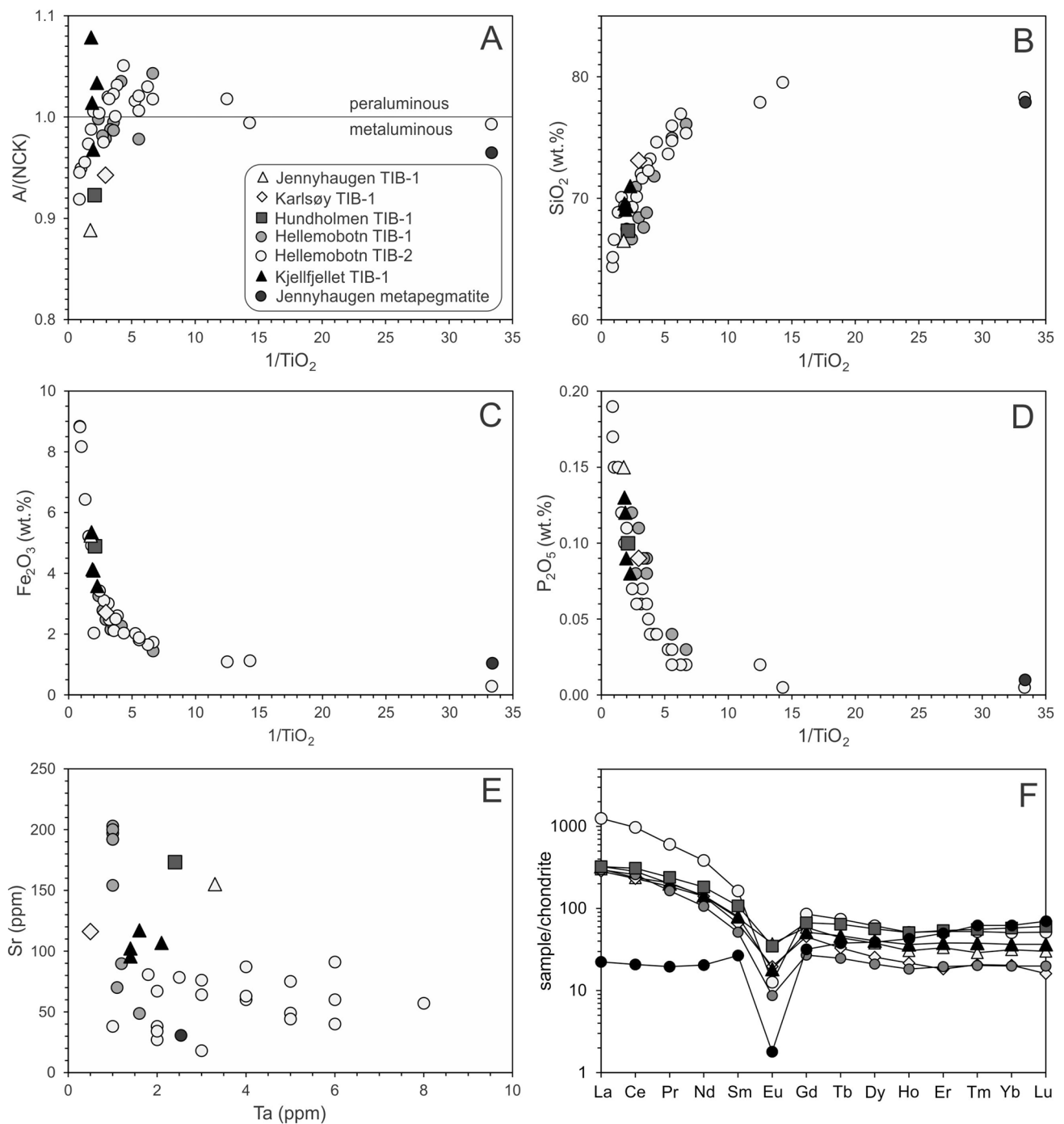


**Fig. 5** Variation diagrams, using  $1/\text{TiO}_2$  as differentiation index, for selected major and trace element components of Tysfjord granite gneiss and the Jennyhaugen metapegmatite (wall zone) exposed in the northern Tysfjord window

### Karlsøy (sample 3122)

Five single, euhedral zircon prisms were analysed from this sample (analyses 610/6 to 610/10). Two zircon crystals have a medium aspect ratio (1:3 to 1:4) and are highly metamict (610/6 and 610/7). After chemical abrasion, only the outer parts of the zircon crystals were left. These grains display

faintly visible oscillatory zonation in the metamict central parts of the grains and either faint oscillatory zonation or homogeneous zones at the margin. The remaining zircon crystals have a medium to high aspect ratio (1:3–1:5) and show oscillatory to sector zoning. All analyses are discordant with the oscillatory zoned, high aspect ratio zircon crystals being the least discordant ones and the metamict zircon



crystals being the most discordant ones. The analyses do not define a single discordia line, indicating that two or more post protolith crystallisation Pb-loss events or recrystallization events affected the zircons. The least discordant analysis (610/8) still constrains the protolith age. If analysis 610/8 is combined with the youngest, metamict zircon, an upper intercept age of  $1804.7 \pm 1.0$  Ma ( $2\sigma$ ) is obtained, with a lower intercept age of  $433.7 \pm 4.5$  Ma ( $2\sigma$ ). The upper intercept age is considered the best estimate for the protolith age of this phase of the Tysfjord granite gneiss, while the lower intercept age corresponds to the age of Scandian metamorphism (e.g., Grimmer et al. 2015).

The best estimates of protolith ages for both Tysfjord granite gneisses,  $1801 \pm 6$  Ma (Jennyhaugen) and  $1804.7 \pm 1.0$  Ma (Karlsøy), cannot resolve age differences between the two phases and, thus, a common age of ca. 1805 Ma is suggested. Based on the zircon data, the timing of Caledonian metamorphism cannot be resolved. High-temperature metamorphism during the Caledonian Orogeny is, however, here interpreted to result in zircon recrystallisation that led to the observed post-Scandian Pb mobilisation.

### Tjeldøya pegmatite zircon U–Pb dating

A fragment broken off from one large, pristine, moderately metamict zircon from the Tjeldøya pegmatite was analysed (Fig. 6D). The zircon has a low Th/U-ratio of 0.043 and is concordant at  $392.87 \pm 0.84$  Ma ( $2\sigma$ ; MSWD (of concordance) = 0.97), which we interpret to represent the crystallisation of zircon from the pegmatite melt and, hence, the emplacement of the pegmatite.

### Tysfjord (meta-)pegmatite columbite-group mineral chemistry

The complete list of major and minor element concentrations of columbite-group minerals selected for dating is provided in the Supplementary Material Table SM2. The dated columbite-group minerals plot as columbite–(Fe) and columbite–(Mn) according to the Mn/(Mn + Fe) versus Ta/(Ta + Nb) discrimination diagram of Černý (1989) (Fig. 7). Some Tysfjord columbite crystals are among the lowest Ta columbite-tantalite group minerals from Svecofennian NYF pegmatites. Columbite from undeformed Group 2 pegmatites has, however, higher Ta/(Ta + Nb) ratios due to higher Ta and lower Nb than Group 1 columbite and shows little variation in Mn/(Mn + Fe). In contrast, Group 1 columbite is characterised by highly variable Mn/(Mn + Fe) ratios and similar Ta/(Ta + Nb) ratios. Based on the Nb and Ta contents, Group 1 metapegmatites and Group 2 pegmatites are well distinguishable. The Sn, W, Ti, and Zr contents of both groups are low, and REE, Y, and U are commonly below the limit of detection. Only columbite–(Mn) from Tjeldøya has

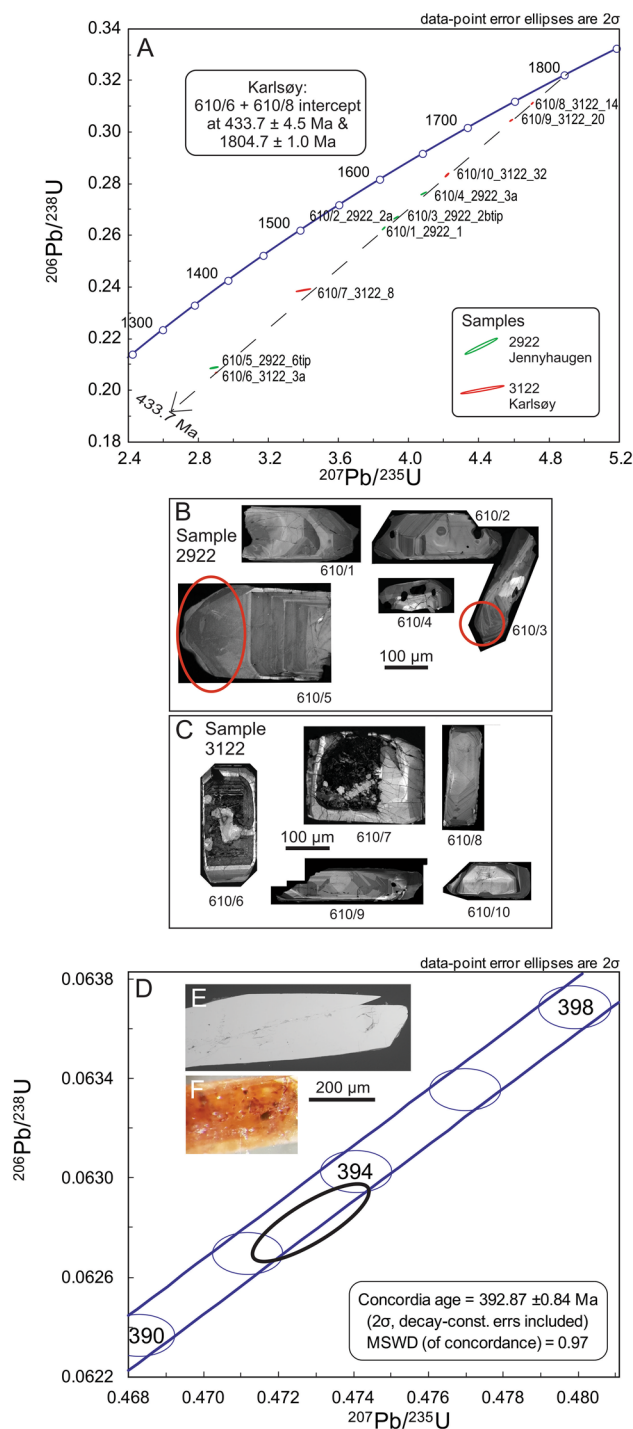


**Fig. 6** **A** Concordia diagram for zircon from two Tysfjord granite gneisses (samples 2922 and 3122) analysed in this study. Error ellipses are plotted with  $2\sigma$  absolute errors (including decay constant errors). Sample locations are shown in Fig. 1. **B** and **C** SEM-CL images of analysed zircon crystals of samples 2922 and 3122. **D** Concordia diagram displaying the analysis of a fragment of the Tjeldøya pegmatite zircon. **E** BSE image of the analysed zircon. **F** Optical image of the central part of the zircon. Note the brown color and slightly foggy appearance reflecting metamictisation, and the presence of inclusions. Sample location is shown in Fig. 1

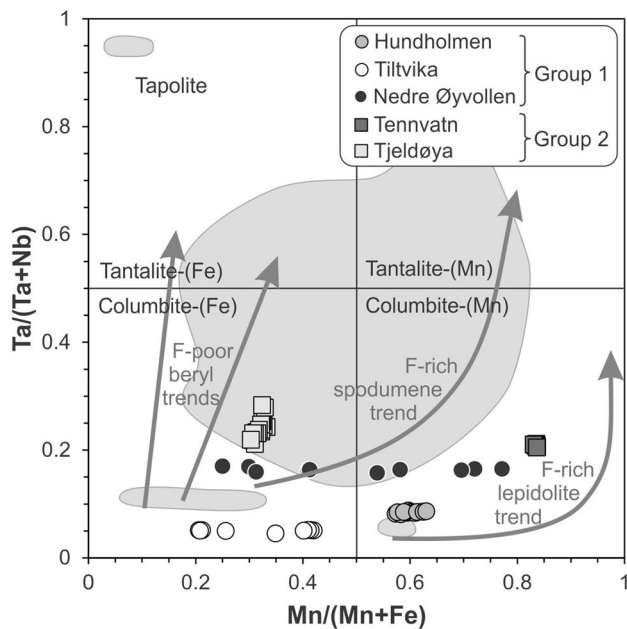


**Fig. 7** Quadrilateral classification diagram (according to Černý 1989) shows the chemical variation of columbite-group minerals used for dating of Tysfjord (meta-)pegmatites. The grey fields indicate the compositional variation of columbite-group minerals from Svecofenian NYF pegmatites of Sweden and southern Finland based on data from Romer and Smeds (1994, 1997), Lindroos et al. (1996), Romer (1997), and Müller et al. (2017). The chemical evolution trends are according to Černý (1989)

elevated Ti concentrations. The very low Sn and W contents (see also Melcher et al. 2016) seems to reflect the limited availability of Sn and W, rather than the restricted possibility to incorporate them (see also Tysfjord granite gneiss chemistry).

### Tysfjord (meta-)pegmatite U–Pb columbite dating

Data from the five dated columbite samples fall on a discordant trend between early Proterozoic and early Paleozoic ages. Two samples give concordant data with early Paleozoic ages, whereas the data from three Paleoproterozoic columbite samples define a discordant trend (Fig. 8). The data show that there are two crystallization events of columbite-group minerals.

#### Hundholmen (annealed)

Four fragments of a columbite crystal from the Hundholmen metapegmatite have been analyzed. The samples were annealed and leached before dissolution. The leached samples are characterized by relatively low U (55–99 ppm) and Pb (20–34 ppm) contents, which possibly indicate that during recrystallization of columbite, U was preferentially incorporated in a separate phase that readily dissolved

during leaching or the leaching could have non-systematically fractionated U and Pb, resulting in variable degrees of U and Pb loss. All fragments had relatively high common Pb contents of 0.92–3.6 ppm, resulting in relatively low measured  $^{206}\text{Pb}/^{204}\text{Pb}$  ratios (Table 1). The analytical results define a discordant trend that intersects the concordia line at  $1755.9 \pm 4.9$  Ma ( $2\sigma$ , MSWD=0.16) and  $404 \pm 28$  Ma ( $2\sigma$ ). The upper intercept is interpreted as the age of columbite crystallization and, thus, pegmatite emplacement at ca. 1756 Ma, whereas the lower intercept reflects recrystallization and/or Pb loss during the Caledonian orogeny. The dates show clearly, that the columbite is of Paleoproterozoic age and recrystallized during the Caledonian orogeny.

#### Tiltvika (annealed)

Columbite from Tiltvika was annealed before analysis. The leached four fragments are characterized by relatively low U (33–82 ppm) and Pb (14–34 ppm), have common Pb contents of 0.35–0.96 ppm, and relatively radiogenic  $^{206}\text{Pb}/^{204}\text{Pb}$  ratios (Table 1). The data plot to both sides of the concordia and define a discordant trend that intercepts at  $1772.4 \pm 2.9$  Ma ( $2\sigma$ , MSWD=0.47) and  $437 \pm 24$  Ma ( $2\sigma$ ) (Fig. 8A). The lower intercept reflects recrystallization and/or Pb loss. As for the Hundholmen metapegmatite, we interpret the upper intercept as the age of pegmatite emplacement and the lower intercept as evidence for recrystallization during the Caledonian orogeny.

#### Nedre Øyvollen

We analyzed six fragments of a columbite crystal from the Drag metapegmatite field. The samples were not annealed before leaching. All fragments are characterized by high U contents (373–625 ppm). All fragments have high common Pb contents (3.3–23.9 ppm) and, therefore, are characterized by low measured  $^{206}\text{Pb}/^{204}\text{Pb}$  ratios (Table 1). The analytical data scatter do not define a discordant trend. In a diagram showing the data from the Drag columbite together with the data from the Hundholmen and Tiltvika columbites, the Drag data plot close to the discordant trend defined by the Hundholmen and Tiltvika columbites (Fig. 8A). The offset of some of the Drag data toward the origin of the diagram reflects post-Caledonian Pb loss. Columbite from Drag does not permit an age interpretation. Because columbite from Drag, Hundholmen, and Tiltvika show similar data distribution, we interpret the data of columbite from Drag to reflect Caledonian recrystallization of a Paleoproterozoic columbite, which lost Pb due to pre-Caledonian metamictisation.

**Fig. 8** U–Pb data for leached columbite-group minerals from Tysfjord (meta-)pegmatite localities Hundholmen, Tennvatn and Tjeldøya. Analytical data are shown at  $2\sigma$  uncertainties. Data from Table 1; for discussion see text. In A, Pb/U ratios of an allanite–(Ce) sample from the Stetind metapegmatite determined by Hetherington et al. (2021) are added. The allanite–(Ce) data indicate an inherited pre-Caledonian age

### Tennvatn

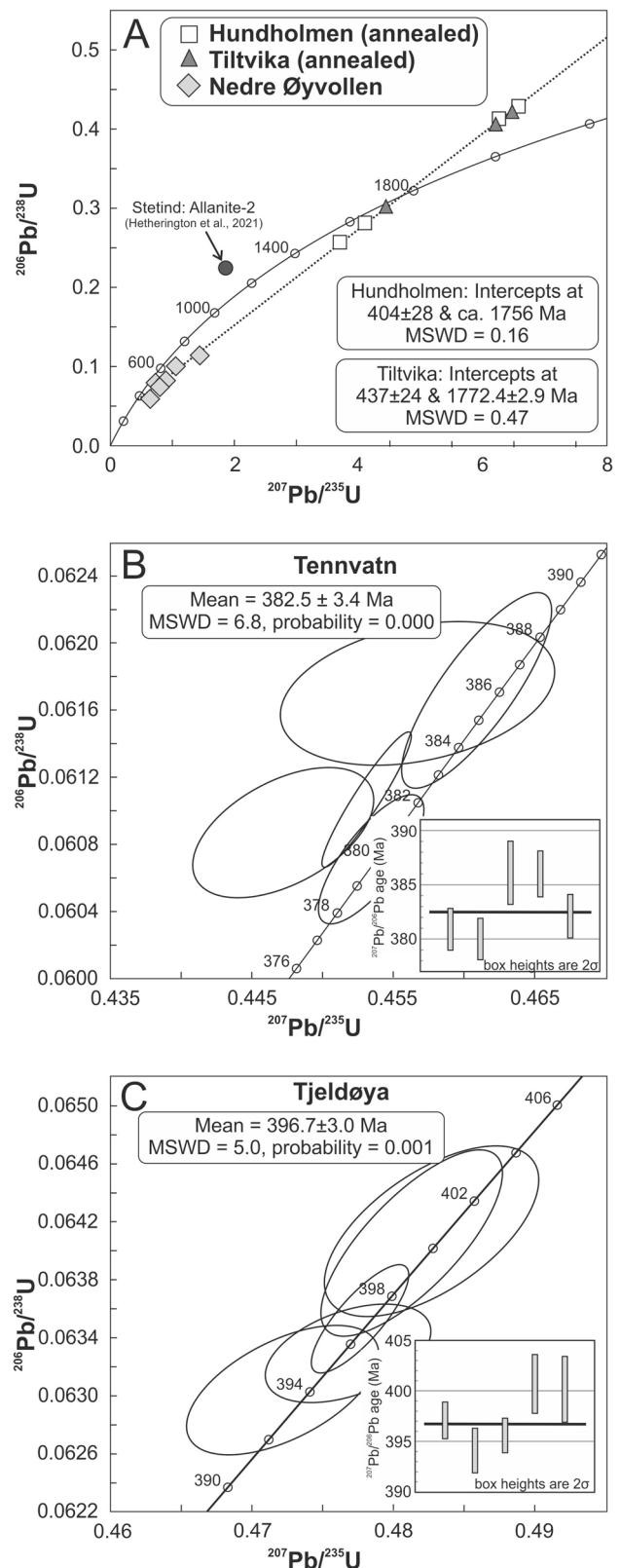
The U–Pb data of five fragments from a columbite crystal from the Tennvatn pegmatite fall on or slightly above the Concordia. The uncertainties do not all overlap within uncertainties. The various fragments have similar U contents (180–213 ppm), but very variable common Pb contents (0.35–6.3 ppm), resulting in a broad range of measured  $^{206}\text{Pb}/^{204}\text{Pb}$  ratios (Table 1). The data show excess scatter and the average of the five  $^{206}\text{Pb}/^{238}\text{U}$  ages yields an age of ca. 383 Ma (Fig. 8B). This age is interpreted to date the crystallization of columbite and the emplacement of the pegmatite.

### Tjeldøya

Five of the six analysed columbite fragments from the Tjeldøya pegmatite are concordant and overlap within analytical uncertainty. The remaining fragment also is concordant, but yields a slightly younger apparent age. Most fractions have low common Pb contents (0.06–0.46 ppm), but one sample has 2.2 ppm common Pb, which may be due to a sulphide or feldspar inclusion. Although there is significant scatter between the individual data points, a weighted average of five overlapping  $^{206}\text{Pb}/^{238}\text{U}$  ages gives an age of ca. 397 Ma. This age is similar to the zircon concordia age ( $392.87 \pm 0.84$  Ma) and corroborates the interpretation of the latter age as dating the emplacement of the pegmatite. The youngest columbite analysis is equal in age, within uncertainty, to the zircon, and the slightly older ages of the remaining concordant columbite analyses probably reflects that the actual common Pb composition was slightly more radiogenic than the Pb isotopic composition used for the common Pb correction. Nevertheless, the data shows that both the columbites and zircon crystallized during emplacement of the pegmatite. Corresponding ages of independent U–Pb columbite and U–Pb zircon dating of the Tjeldøya pegmatite prove the robustness of the applied methods.

## Discussion

Our data demonstrate two regional pegmatite-forming events in the same area and in the same lithological unit. These are related to two orogens: Late Svecofennian Group 1



metapegmatites (1755–1772 Ma) and late Caledonian Group 2 pegmatites (400–379 Ma). In the following, the two events



and their implications for the orogenic evolution and the pegmatite formation in general are discussed.

### Svecofennian magmatism and related Group 1 metapegmatite formation in the Tysfjord area

The Svecofennian granite suite of the northern Tysfjord window is dominated by the older TIB-1 granites as shown by our and previously published data (Romer et al. 1992 and this study). Crystallization ages of these granites vary from 1781 to 1809 Ma. Our data from the northern Hamarøy area (Drag-Finnøy; zircon U–Pb  $1804.7 \pm 3.9/-10.9$  Ma), where the majority of Group 1 metapegmatites occur, also fall in this age range. Occurrences of TIB-2 granites, which form relatively small bodies (several hundred meters in diameter) intruded into TIB-1, seem to be limited to the eastern edge of the pegmatite field and Tysfjord window (Fig. 1).

The U–Pb columbite ages of the Tiltvika and Hundholmen Group 1 metapegmatites hosted by the TIB-1 granites, are  $1772.4 \pm 2.9$  Ma and  $1755.9 \pm 4.9$  Ma, respectively. Note that these U–Pb ages may not be accurate as they were determined on strongly metamict columbite that was annealed before analysis. The sample from Drag shows a similar data distribution as Tiltvika and Hundholmen columbite and, thus, is likely to have a Neoproterozoic formation age, which due to Caledonian recrystallization with associated Pb loss, cannot be determined precisely. The amphibolite-facies Caledonian metamorphism resulted in the partial resetting of the U–Pb systems of zircon and columbite that now define discordant arrays between an early Proterozoic and an early Paleozoic event. Thus, the accuracy and precision of the data should not be overinterpreted. The formation of the Group 1 metapegmatites is likely to be related to the TIB-1 granite emplacement.

The similarity of bulk chemistries of the most evolved TIB granites and the Jennyhaugen metapegmatite strongly implies a genetic link between the Group 1 metapegmatites and TIB granites (Fig. 5). The upper-crust-normalized pattern of the Jennyhaugen metapegmatite is similar to that of the TIB granites except for the lower LREE contents (Fig. 9). The low LREE is caused by crystal fractionation of allanite-(Ce), monazite-(Ce) and fluorapatite (these are the major carriers of the LREE in the TIB granites; Müller 2011) in the analysed wall zone of the Jennyhaugen metapegmatite. The lower Ba, Ti, Sr, Eu and Zr suggest a higher degree of fractionation of the pegmatites than the TIB granites. The mineralogy of the Group 1 metapegmatites characterises them as NYF pegmatites particularly enriched in fluorite and allanite-(Ce) with a chemical A-type granite signature, similar to the TIB granites. Fluorite and allanite-(Ce) are also common accessories of the Tysfjord granite gneiss (Müller 2011).

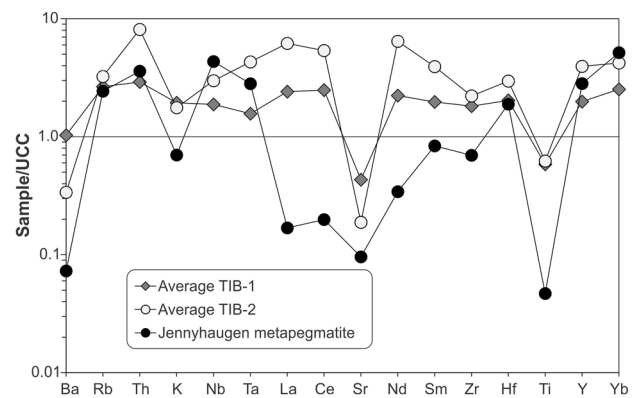


**Fig. 9** Diagram of UCC-normalized trace elements of TIB-1 and TIB-2 granite gneisses of the Tysfjord area and the Jennyhaugen Group 1 metapegmatite (wall zone). UCC values are according to Rudnick and Gao (2004)

The chemical similarity of Group 1 metapegmatites and TIB granite gneisses indicates that the pegmatites could represent residual melts of TIB granites. The extraordinary large size of the Tysfjord metapegmatites of up to several hundred of meters is noteworthy, as intra-plutonic NYF pegmatite typically do not exceed the size of about 10 m as, for example, the pegmatites of Strzegom in Poland (e.g. Janeczek 2007), Erongo in Namibia (Falster et al. 2018), South Platte district in Colorado (e.g. Simmons et al. 1987) and Königshain in Germany (Thomas and Davidson 2016). Exceptions are NYF-type pegmatites related to Proterozoic rapakivi granites in Ukraine (e.g. Lyckberg 2009) and Finland (e.g. Lyckberg 2006), which can be of up to 100 m in size. The large size of the Ukrainian Volodarsk-Volynski chamber pegmatites and Finish Luumäki pegmatite system possibly reflect that the already largely crystallized rapakivi granites behaved as increasingly brittle bodies, facilitating efficient transport of residual melts and the concentration of incompatible elements, such as F, Rb, Ga, Zr, Hf, Th, U, and REE, that had moderate levels in the rapakivi granites (Lyckberg 2009; Michallik et al. 2017). Both the Finish and Ukrainian rapakivi granites share chemical similarities with the Tysfjord and other TIB granites, in particular high F, Th, U and REE contents and overlapping emplacement ages of granites and pegmatites. High F content of the rapakivi granites and Tysfjord granite gneiss may have triggered and enhanced the separation of relatively large volumes of F–H<sub>2</sub>O-enriched melt proportions as suggested by Michallik et al. (2017), which resulted in the crystallization of unusual large granite-melt-derived NYF pegmatites in the Tysfjord area.

## Group 2 pegmatite formation in the context of Caledonian orogenesis (430–390 Ma) of central Scandinavia

The evolution of the Scandinavian Caledonides was accompanied by two major types and phases of magmatism, an older phase related to the nappe stacking and a younger phase related to uplift of the orogen (e.g. Nordgulen, et al. 1993; Larsen et al. 2002; Steltenpohl et al. 2003; Barnes et al. 2007). Magmatism in the vicinity of the Tysfjord basement window was, however, less pronounced than in other parts of the Scandinavian Caledonides.

Granites of the older phase (c. 430–420 Ma) resulted from local migmatization and melt segregation after nappe stacking. Migmatites within the Narvik Nappe Complex formed after the peak metamorphism at  $432 \pm 2$  Ma at conditions of 650–800 °C and  $12 \pm 2$  kbar (Northrup 1997). The  $427 \pm 6$  Ma old Dragvik granite was emplaced across the thrust between the Ofoten and Niingen nappes (Steltenpohl et al. 2003). The originally reported Rb–Sr isochron age of  $427 \pm 6$  Ma (Steltenpohl et al. 2003) was recalculated using the recommended  $^{87}\text{Rb}$  decay constant of  $1.3972 \pm 0.0045$  ( $10^{-11} \text{ a}^{-1}$ ; Villa et al. 2015) to  $435 \pm 6$  Ma. This age, however, does not agree with the observation that the granite cuts the nappe boundaries, because the Ofoten and Niingen nappes were not on top of each other at that time (Steltenpohl et al. 2003). Felsic dykes and small plutons in the Ofoten-Troms region of similar chemical signature and setting as the Dragvik granite have a better constrained age. The emplacement of this suite is dated by the  $425 \pm 1$  Ma age of the Tennes granite that intruded the Balsfjord Group, which overlies the Narvik Nappe Complex (Augland et al. 2014).

The second magmatic phase at c. 400 (– 370) Ma occurred at a time when the Caledonian orogen and its foreland were affected by major crustal extension (e.g., Eide et al. 2002). Within the Caledonides, this regime is expressed in the form of extensional reactivation of the basal detachment zones and the exhumation of high- and ultrahigh-grade rocks, today exposed as basement windows in western Norway. The extension reactivated also other thrusts and faults, as for example, the N-S striking structures that were active during the formation of the antiformal stacks of basement rocks that formed during the Caledonian continent–continent collision (e.g. Romer et al. 1994; Eide et al. 2002; Wiest et al. 2020). Reactivation of these structures controlled the orientation of the Group 2 pegmatites between 400 and 379 Ma and provided the conduits for melts and/or fluids that facilitated local melting. In the Tysfjord area, temperatures were at least 550 to 650 °C during extensional shearing at  $395 \pm 5$  Ma (U–Pb titanite age; Gromet and Andresen 1993) at the basal contact of the Narvik Nappe Complex and the

Tysfjord granite gneiss at Etfjord. Gromet and Andresen (1993) interpreted the 395 Ma age to date the formation of the main foliation along the basement–metasediment contact and in the Tysfjord granite gneiss. For a geothermal gradient of 30–40 °C/km, this temperature of 550–650 °C corresponds to a pressure of 3.5–6.5 kbar. At these P–T conditions, fluid-present shear-related partial melting of rocks near the regional detachment horizon could generate the pegmatite melts (e.g. Brown and Korhonen 2009).

The chemistry and mineralogy of Group 2 pegmatites and the Tysfjord granite gneisses are broadly similar. Therefore, the pegmatite melts are interpreted as products of local partial melting of the Tysfjord granite gneisses, which is in line with the absence of coeval granites that could serve as source for the pegmatite melts in the central Scandinavian Caledonides. The Tysfjord granite gneisses are poor in B and granite-derived Group 1 metapegmatites rarely have tourmaline (there is a single sample of schorl and luinaite-(OH) from a late fracture in the Hundholmen metapegmatite; Kolitsch et al. 2011). Therefore, abundant tourmaline (Fe-rich fluor-schorl; Kolitsch et al. 2011) in Group 2 pegmatites indicates influx of B, possibly from the B-rich metasediments overthrust by the basement nappes. Tourmaline is known from the metasedimentary rocks of the lower nappes, for example, from Slunkajavrr (Fig. 1B; Mindat 2021). The structure of the Strindfjellet Bend provides evidence that the Tysfjord granite gneiss was overthrust over Caledonian metasediments in the Tennvatn–Slunkavarre–Hellmobotn area and, thus, metasediments occur at depth, below the granite gneiss. Because the pegmatite melts were emplaced along N–S-trending extensional fractures, metasediment-derived metamorphic B-enriched fluids might have circulated along these fractures. These fluids may have lowered locally the melting temperature of the Tysfjord granite gneiss (e.g. Chorlton and Martin 1978). According to Chorlton and Martin (1978), the addition of B to a water-saturated granitic system lowers the solidus and partial melting point at 1 kbar by 125 °C to about 600 °C.

Hetherington et al. (2021) reported a combined 410–400 Ma age (U–Pb zircon, allanite-(Ce), fergusonite-(Y), uraninite) for the Stetind pegmatite confirming our Caledonian ages of Group 2 pegmatites. Hetherington et al. (2021) interpret the age as the crystallization age of the pegmatite, which resulted from anatexis of the Tysfjord granite gneiss. We were not able to obtain reliable data for the Stetind pegmatite. Field observations, however, clearly indicate that this pegmatite, which is strongly deformed and recrystallized, belong to the Paleoproterozoic Group 1 of metapegmatites (Fig. 10).

The dated minerals contain several wt% U (Table 2 in Hetherington et al. (2021)). If they were Paleoproterozoic minerals, they were metamict at the time of the Caledonian orogeny and may have recrystallized during the Caledonian

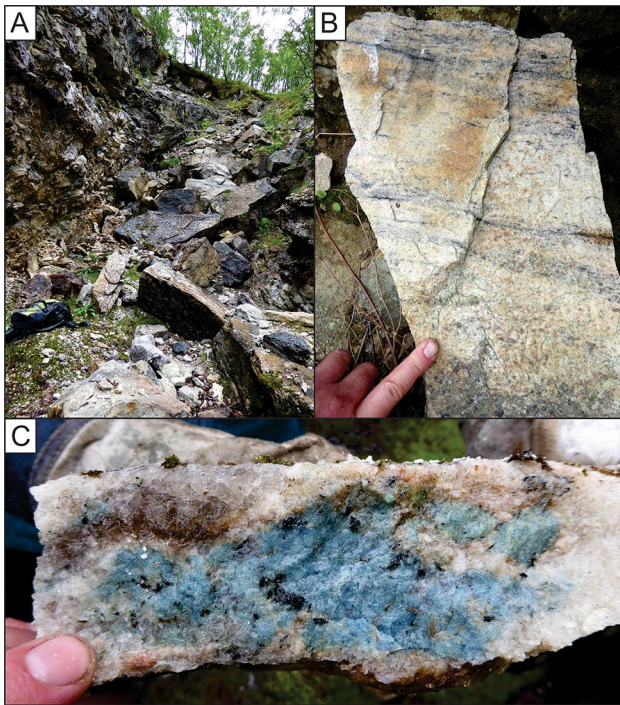


**Fig. 10** Field photographs of the Stetind metapegmatite. **A** Stetind metapegmatite quarry filled with pegmatite blocks. Due to the strong Caledonian foliation, the metapegmatite splits into platy blocks along foliation planes that are coated with recrystallized biotite. **B** Strongly foliated wall zone of the Stetind metapegmatite. The foliation planes are marked by recrystallized biotite and quartz. **C** Sheared, fragmented and recrystallized blue beryl in a recrystallized quartz–feldspar matrix

metamorphism excluding Pb from the recrystallized crystal lattice. Such a reinterpretation of the Hetherington et al. (2021) data agrees with one allanite–(Ce) sample (allanite-2 in Table 2 of Hetherington et al. 2021) that has high  $^{206}\text{Pb}/^{238}\text{U}$  and  $^{207}\text{Pb}/^{235}\text{U}$  ratios of 0.22784 and 1.83201, respectively, which correspond to older pre-Caledonian apparent ages and provides evidence for inherited radiogenic Pb from older allanite (cf. Figure 8A). Note, the Stetind allanite falls above the Concordia line to the right of a line through the Caledonian age of 400 Ma of these samples and the origin of the diagram (Fig. 8A), which implies that (1) there was some post 400 Ma U and Pb mobility and (2) allanite-2 contains inherited radiogenic Pb from a precursor mineral. Therefore, the age provided by Hetherington et al. (2021) represents the age of metamorphism rather than the age of pegmatite formation.

So far, three Group 2 pegmatite localities are known from the northern Tysfjord basement window: Tennvatn, Hellmobotn and Tjeldøya (Fig. 1B). These pegmatites occur in an area of  $80 \times 30$  km and, thus, show remelting of the Tysfjord granite gneisses is not a local event. Actually, similar pegmatites involving partial melting of the Svecofennian

basement and nappe footwall rocks are also known from other, tectonic windows in the central Scandinavian Caledonides to the southwest of the Tysfjord window. Larsen et al. (2002) described decompression-related migmatization at  $398 \pm 2$  Ma and pegmatite melt formation at  $403 \pm 3$  Ma from the Sjona window and the emplacement of pegmatite melts at  $409 \pm 5$  Ma at the nappe footwall on Træna islands (Fig. 1). These partial melting events are related to top-W to -SW ductile extensional shearing and sinistral strike-slip associated with decompression melting and dome formation during nappe stack unroofing (Larsen et al. 2002). Such a regime is of regional significance (Eide et al. 2002; Braathen et al. 2002; Dewey and Strachan 2003; Osmundsen et al. 2003) and seems to have affected the entire central Scandinavian Caledonides, including the Tysfjord area. Remarkably, the age of the shear-related partial melting decreases from about 410–400 Ma at Træna–Sjona in the southwest to 400–379 Ma at Tysfjord.

## Conclusions

Age data of the granite and (meta-)pegmatite suite exposed in the northern Tysfjord tectonic window reveal that there are two age groups of rare element NYF-type pegmatites that have similar chemical and mineralogical signatures, but different size, structure and deformation degree: the late Svecofennian Group 1 metapegmatites and the late Caledonian Group 2 pegmatites. Group 1 metapegmatites and their hosting granites have similar ages, indicating that the pegmatites formed from residual melts of the hosting granite, which is supported by the similar bulk chemical composition of Group 1 metapegmatites and granites. Group 1 NYF-type metapegmatites form extraordinary large bodies (up to 400 m), which may reflect the overall high F contents of the hosting granites that facilitated the late-stage separation of relatively large volumes of F–H<sub>2</sub>O-enriched melts. Group 1 metapegmatites were metamorphosed and deformed during amphibolite facies Caledonian metamorphism.

Group 2 pegmatites are much smaller. They are undeformed and are interpreted to have formed from fluid-present shear-related partial melting of the Tysfjord granite gneiss during late stages of the Caledonian orogeny between 400 and 379 Ma. The high B content of Group 2 pegmatites indicate that external B-rich fluids from Caledonian metasedimentary rocks, which were overthrust by the Tysfjord granite gneiss, may have fluxed melting along reactivated N–S striking structures. On the regional scale, partial melting was related to top-W to top-SW ductile extensional shearing of the central Scandinavian Caledonides.

**Supplementary Information** The online version contains supplementary material available at <https://doi.org/10.1007/s00531-022-02166-5>.



**Acknowledgements** This study is funded by European Commission's Horizon 2020 innovation programme under Grant agreement no. 869274, project GREENPEG New Exploration Tools for European Pegmatite Green-Tech Resources. We highly appreciate the constructive comments of Reinhard Greiling to the manuscript. We would like to thank Astrid Haugen for providing the columbite crystal from the Tennvatn pegmatite used for U–Pb dating. We thank Brent Miller and Rune Larsen for careful and constructive reviews and Wolf-Christian Dullo for thoughtful editorial handling.

**Funding** Open access funding provided by University of Oslo (incl Oslo University Hospital).

**Open Access** This article is licensed under a Creative Commons Attribution 4.0 International License, which permits use, sharing, adaptation, distribution and reproduction in any medium or format, as long as you give appropriate credit to the original author(s) and the source, provide a link to the Creative Commons licence, and indicate if changes were made. The images or other third party material in this article are included in the article's Creative Commons licence, unless indicated otherwise in a credit line to the material. If material is not included in the article's Creative Commons licence and your intended use is not permitted by statutory regulation or exceeds the permitted use, you will need to obtain permission directly from the copyright holder. To view a copy of this licence, visit <http://creativecommons.org/licenses/by/4.0/>.

## References

- Agyei-Dwarko N, Augland LE, Andresen A (2012) The Heggvatn supracrustals, North Norway—a late Mesoproterozoic to early Neoproterozoic (1050–930 Ma) terrane of Laurentian origin in the Scandinavian Caledonides. *Precambrian Res* 212–213:245–262
- Åmli R (1975) Råstoffundersøkelse i Nord-Norge. Kvarts- og feltspatundersøkelse i Tysfjord og Hamarøy kommuner. In: Norges Geologiske Undersøkelse Rapport Nr. 1358/1
- Anderson MW, Barker AJ (1999) Caledonian terrane analysis in Troms-Tornetrask, northern Scandinavia, utilizing the geochemistry of highlevel metabasites. *Nor Geol Tidsskr* 79:145–159
- Andresen A, Steltenpohl M (1994) Evidence for ophiolite obduction, terrane accretion and polyorogenic evolution of the north Scandinavian Caledonides. *Tectonophysics* 231:59–70
- Andresen A, Tull JF (1986) Age and tectonic setting of the Tysfjord gneiss granite, Eufjord, North Norway. *Nor Geol Tidsskr* 66:69–80
- Augland LE, Andresen A, Corfu F, Agyei-Dwarko NY, Larionov AN (2013) The Bratten–Landegode gneiss complex: a fragment of Laurentian continental crust in the Uppermost Allochthon of the Scandinavian Caledonides. In: Corfu F, Gasser D, Chew DM (eds) *New Perspectives on the Caledonides of Scandinavia and Related Areas*, Geological Society, London, Special Publications, vol 390, pp 633–654. <https://doi.org/10.1144/SP390.1>
- Augland LE, Andresen A, Gasser D, Steltenpohl MG (2014) Early Ordovician to Silurian evolution of exotic terranes in the Scandinavian Caledonides of the Ofoten–Troms area – terrane characterization and correlation based on new U–Pb zircon ages and Lu–Hf isotopic data. In: Corfu F, Gasser D, Chew DM (eds) *New Perspectives on the Caledonides of Scandinavia and Related Areas*, Geological Society, London, Special Publications, vol 390, pp 655–678. <https://doi.org/10.1144/SP390.19>
- Ballo EG, Augland LE, Hammer Ø, Svensen HH (2019) A new age model for the Ordovician (Sandbian) K-bentonites in Oslo, Norway. *Paleogeogr Paleoclimatol Paleoecol* 520:203–213
- Barker A (1986) The geology between Salangsdalen and Gratangenfjord, Troms, Norway. *Norges Geol Undersokelse Bull* 405:41–56
- Barnes CG, Frost CD, Yoshinobu AS, McArthur K, Barnes MA, Allen CM, Nordgulen Ø, Prestvik T (2007) Timing of sedimentation, metamorphism, plutonism in the Helgeland Nappe Complex, north-central Norwegian Caledonides. *Geosphere* 3(6):683–703
- Barros R, Menuge JF (2016) The origin of spodumene pegmatites associated with the Leinster granite in Southeast Ireland. *Can Mineral* 54:847–862
- Bartley JM (1981) Limited basement involvement in Caledonian Deformation, Hinnøy, north Norway, and tectonic implications. *Tectonophysics* 83:85–203
- Bartley JM (1984) Caledonian structural geology and tectonics of east Hinnøy, north Norway. *Norges Geol Unders Bull* 396:1–124
- Baumgartner R, Romer RL, Moritz R, Sallet R, Chiaradia M (2006) Columbite-tantalite pegmatites from the Seridó Belt, NE Brazil: genetic constraints from U–Pb dating and Pb isotopes. *Can Mineral* 44:69–86
- Bergh S, Kullerud K, Myhre PI, Corfu F, Armitage PEB, Zwaan KB, Ravna EJK (2014) Archaean elements of the basement outliers west of the Scandinavian caledonides in northern Norway: architecture, evolution and possible correlation with fennoscandia. In: Dilek Y, Furnes H (eds) *Evolution of archaean crust and early life*. Springer, Berlin, pp 103–112
- Binns RE (1978) Caledonian nappe correlation and orogenic history in Scandinavia north of lat. 67°N. *Geol Soc Am Bull* 89:1475–1490
- Björklund L (1989) Geology of the Akkajaure–Tysfjord–Lofoten traverse, N. Scandinavian Caledonides. In: PhD thesis, Chalmers Tekniska Högskola och Göteborgs Universitet, Publ. A 59, Gothenburg, Sweden.
- Bowring JF, McLean NM, Bowring SA (2011) Engineering cyber infrastructure for U–Pb geochronology: Tripoli and U–Pb Redux. *Geochem Geophys Geosyst* 12:Q0AA19. <https://doi.org/10.1029/2010GC003479>
- Boyd R (1983) The Lillevik dike complex, Narvik: geochemistry and tectonic implications of a probable ophiolitic fragment in the Caledonides of the Ofoten region, North Norway. *Norsk Geol Tidsskrift* 63:39–54
- Braathen A, Osmundsen PT, Nordgulen Ø, Roberts D, Meyer GB (2002) Orogen-parallel extension of the Caledonides in northern Central Norway: an overview. *Norw J Geol* 82:225–241
- Brown M, Korhonen FJ (2009) Some remarks on melting and extreme metamorphism of crustal rocks. In: Dasgupta S (ed) *Physics and chemistry of the earth*. Indian National Science Academy by Springer, New York, pp 67–87
- Burt DM (1989) Compositional and phase relations among rare earth element minerals. In: Lipin BR, McKay GA (eds) *Geochemistry and mineralogy of rare earth elements*. Reviews in mineralogy, vol 21, pp 259–307
- Černý P (1989) Characteristics of pegmatite deposits of tantalum. In: Möller P (ed) *Lanthanides, tantalum, and niobium*. Springer, Berlin, pp 195–239
- Černý P (1991) Rare-element granitic pegmatites. II. Regional to global environments and petrogenesis. *Geosci Can* 18:68–81
- Černý P, Ercit TS (2005) Classification of granitic pegmatites revisited. *Can Mineral* 43:2005–2026
- Chorlton LB, Martin RF (1978) The effect on boron on the granite solidus. *Can Mineral* 16:239–244
- Condon DJ, Schoene B, McLean NM, Bowring SA, Parrish RR (2015) Metrology and traceability of U–Pb isotope dilution geochronology (EARTHTIME Tracer Calibration Part I). *Geochim Cosmochim Acta* 164:464–480

- Corfu F (2004) U-Pb Age, setting and tectonic significance of the anorthosite–mangerite–charnockite–granite suite, Lofoten–Vesterålen, Norway. *J Petrol* 45:1799–1819
- Corfu F, Andersen TB, Gasser D (2014) The Scandinavian Caledonides: main features, conceptual advances and critical questions. In: Corfu F, Gasser D, Chew DM (eds) *New perspectives on the Caledonides of Scandinavia and Related Areas*, Geological Society, London, Special Publications, vol 390, pp 9–43. <https://doi.org/10.1144/SP390.25>
- Crowley PD (1985) The structural and metamorphic evolution of the Sitas area, northern Norway and Sweden. In: PhD thesis, Massachusetts Institute of Technology, Cambridge
- Dewey JF, Strachan RA (2003) Changing Silurian–Devonian relative plate motion in the Caledonides: sinistral transpression to sinistral transtension. *J Geol Soc* 160:219–229. <https://doi.org/10.1144/0016-764902-085>
- Eide EA, Osmundsen PT, Meyer GB, Kendrick MA, Corfu F (2002) The Nesna Shear Zone, north-central Norway: an  $^{40}\text{Ar}/^{39}\text{Ar}$  record of Early Devonian–Early Carboniferous ductile extension and unroofing. *Norwegian J Geol* 82:317–339
- Falster AU, Simmons WB, Webber KL, Boudreaux AP (2018) Mineralogy and Geochemistry of the Erongo Sub-Volcanic Granite–Miarolitic–Pegmatite Complex, Erongo, Namibia. *Can Mineral* 56:425–449
- Fei G, Menuge JF, Li Y, Yanga J, Deng Y, Chen C, Yang Y, Yang Z, Qin L, Zheng L, Tang W (2020) Petrogenesis of the Lijiangou spodumene pegmatites in Songpan–Garze Fold Belt, West Sichuan, China: evidence from geochemistry, zircon, cassiterite and coltan U–Pb geochronology and Hf isotopic compositions. *Lithos* 364–365:105555
- Fossen H (2010) Extensional tectonics in the North Atlantic Caledonides: a regional view. In: Law RD, Butler RWH, Holdsworth RE, Krabbedam M, Strachan RA (eds) *Continental tectonics and mountain building: the legacy of peach and horne*. Geological Society, London, Special Publications, vol 335, pp 767–793
- Fuchsloch WC, Nex PAM, Kinnaird JA (2018) Classification, mineralogical and geochemical variations in pegmatites of the Cape Cross–Uis pegmatite belt, Namibia. *Lithos* 296:79–95
- Garate-Olave I, Müller A, Roda-Robles E, Gil-Crespo PP, Pesquera A (2017) Extreme fractionation in a granite–pegmatite system documented by quartz chemistry: The case study of Tres Arroyos (Central Iberian Zone, Spain). *Lithos* 286–287:162–174. <https://doi.org/10.1016/j.lithos.2017.06.009>
- Gee DG, Sturt BA (1985) *The Caledonide Orogen–Scandinavia and related areas*. Wiley, New York
- Gee DG, Fossen H, Henriksen N, Higgins AK (2008) From the early paleozoic platforms of Baltica and Laurentia to the Caledonide Orogen of Scandinavia and Greenland. *Epsides* 31:44–51
- Gee DG, Stephens MB (2020) Lower thrust sheets in the Caledonide orogen, Sweden: Cryogenian–Silurian sedimentary successions and underlying, imbricated, crystalline basement. In: Stephens MB, Bergman Weihed J (eds) *Sweden: Lithotectonic framework, tectonic evolution and mineral resources*, Geological Society, London, Memoirs, vol 50, pp 495–515. <https://doi.org/10.1144/M50-2018-7>
- Gorbatshev R (1985) Precambrian basement of the Caledonides. In: Gee DG, Sturt BA (eds) *The Caledonide Orogen—Scandinavia and related areas*. Wiley, Chichester, pp 197–212
- Greiling RO, Gayer RA, Stephens MB (1993) A basement culmination in the Scandinavia Caledonides formed by antiformal stacking (Bångonåve, northern Sweden). *Geol Mag* 130:471–482
- Griffin WL, Taylor PN, Hakkinen JW, Heier KS, Iden IK, Krogh EJ, Malm O, Olesen KI, Ormaasen DE, Tveten E (1978) Archean and Proterozoic evolution of Lofoten–Vesterålen, N Norway. *J Geol Soc Lond* 135:629–647
- Grimmer JC, Glodny J, Drüppel K, Greiling RO, Kontny A (2015) Early- to mid-Silurian extrusion wedge tectonics in the central Scandinavian Caledonides. *Geology* 43:347–350. <https://doi.org/10.1130/G36433.1>
- Gromet LP, Andresen A (1993) U–Pb age constrains on Caledonian shear strain developed at the basement–allochthon contact, Ofoten region, Norway. *EOS, Transaction American Geophysical Union* 74/16, Spring Meeting Suppl, p 123
- Hetherington CJ, Mailloux GA, Miller BV (2021) A multi-mineral U–(Th)–Pb dating study of the Stetind pegmatite of the Tysfjord region, Norway, and implications for production of NYF-rare element pegmatites during orogenic collapse. *Lithos* 398–399:106257
- Hodges KV (1985) Tectonic stratigraphy, and structural evolution of the Etfjord–Sitasjaure area, North Scandinavian Caledonides. *Norges Geol Unders Bull* 399:41–62
- Hodges KV, Royden L (1984) Geologic thermobarometry of retrograded metamorphic rocks—an indication of the uplift trajectory of a portion of the northern Scandinavian Caledonides. *J Geophys Res* 89:7077–7090
- Hodges KV, Bartley JM, Burchfiel BC (1982) Structural evolution of an A-type subduction zone, Lofoten–Rombak area, northern Scandinavian Caledonides. *Tectonics* 1:441–462
- Hodges KV (1982) Tectonic evolution of the Aesfjord–Sitas area, Norway–Sweden. In: PhD thesis, Massachusetts Institute of Technology, Cambridge
- Högdahl K, Andersson UB, Eklund O (2004) The Transscandinavian Igneous Belt (TIB) in Sweden: a review of its character and evolution. In: *Geological Survey of Finland, Special Paper*, vol 37, p 125
- Husdal T (2008) The minerals of the pegmatites within the Tysfjord granite, northern Norway. *Norsk Bergverksmuseum Skrift* 38:5–28
- Huyskens MH, Zink S, Amelin Y (2016) Evaluation of temperature-time conditions for the chemical abrasion treatment of single zircons for U–Pb geochronology. *Chem Geol* 438:25–35
- Ilickovic T, Schuster R, Mali H, Onuk P, Horschneegg M (2017) Genesis of spodumene pegmatites in the Austroalpine unit (Eastern Alps): isotopic and geochemical investigations. In: *8th international symposium on granitic Pegmatites, Kristiansand, Norway*, NGF Abstracts and Proceedings, vol 2, pp 54–57
- Jaffey AH, Flynn KF, Glendenin LE, Bentley WC, Essling AM (1971) Precision measurements of half-lives and specific activities of  $^{235}\text{U}$  and  $^{238}\text{U}$ . *Phys Rev C* 4:1889–1906
- Janeczek J (2007) Intragranitic pegmatites of the Strzegom–Sobotka massif—an overview. *Granitoids Poland AM Monogr* No 1:193–201
- Karlsen TA (2000) Economic potential of potassic feldspar-rich gneisses in Tysfjord/Hamarøy, northern Norway. *Norges Geol Unders Bull* 436:129–135
- Kirkland CL, Daly JS, Chew DM, Page LM (2008) The Finnmarkian Orogeny revisited: an isotopic investigation in eastern Finnmark, Arctic Norway. *Tectonophysics* 460:158–177
- Knoll T, Schuster R, Huet B (2018) Spodumene pegmatites and related leucogranites from the Austroalpine Unit (Eastern Alps, Central Europe): field relations, petrography, geochemistry and geochronology. *Can Mineral* 56:489–528
- Kolitsch U, Husdal TA, Brandstätter F, Ertl A (2011) New crystal-chemical data for members of the tourmaline group from Norway: occurrences of fluor-schorl and luinaite-(OH). *Norsk Bergverksmuseum Skrift* 46:17–24
- Konzett J, Schneider T, Nedyalkova L, Hauzenberger C, Melcher F, Gerdes A, Whitehouse M (2018) Anatectic granitic pegmatites from the Eastern Alps: a case of variable rare-metal enrichment during high-grade regional metamorphism—I: mineral

- assemblages, geochemical characteristics, and emplacement ages. *Can Mineral* 56:555–602
- Kroner U, Stephan T, Romer RL, Roscher M (2020) Paleozoic plate kinematics during the Pannotia-Pangaea supercontinent cycle. *Geol Soc Lond Spec Publ* 503:83–104
- Lahtinen R, Garde AA, Melezhik VA (2008) Paleoproterozoic evolution of Fennoscandia and Greenland. *Episodes* 31:20–28
- Lahtinen R, Korja A, Nironen M, Heikkinen P (2009) Palaeoproterozoic accretionary processes in Fennoscandia. In: Cawood PA, Kröner A (eds) *Earth accretionary systems in space and time*. The Geological Society, London, Special Publications, vol 318, pp 237–256
- Larsen Ø, Skår Ø, Pedersen R-B (2002) U-Pb zircon and titanite geochronological constraints on the late/post-Caledonian evolution of the Scandinavian Caledonides in north-central Norway. *Nor Geol Tidsskr* 82:1–13
- Lindroos A, Romer RL, Ehlers C, Alviola R (1996) Late-orogenic Svecofennian deformation in SW Finland constrained through pegmatite emplacement ages. *Terra Nova* 8:567–574
- Lindstrøm M (1988) Rb-Sr geokronologi av prekambriske og kaledonske bergarter i Ofoten og Troms. PhD thesis, University of Tromsø, Norway
- London D (2008) Pegmatites. *Can Mineral Spec Publ* 2008:10
- Ludwig KR (2003) User's manual for ISOPLOT 3.00: a geochronological toolkit for Microsoft Excel. Berkeley Geochronol Center Spec Publ 4:4
- Lyckberg P (2006) Mirolitic pegmatites of the Viborg rapakivi granite massif, SE Finland with special attention to the green gem beryl producing Karelia Beryl Mine pegmatite at Luumäki, Karelia. *Norsk Bergverksmuseum Skrift* 33:87–107
- Lyckberg P (2009) Volodarsk—Volynski Chamber Pegmatites. *Mineral Rec* 40:473–506
- Mattinson JM (2005) Zircon U-Pb chemical abrasion (“CA-TIMS”) method: combined annealing and multi-step partial dissolution analysis for improved precision and accuracy of zircon ages. *Chem Geol* 220:47–66
- Melcher F, Graupner T, Gäbler H-E, Sitnikova M, Oberthür T, Gerdes A, Badanina E, Chudy T (2016) Mineralogical and chemical evolution of tantalum–(niobium–tin) mineralisation in pegmatites and granites. Part 2: Worldwide examples (excluding Africa) and an overview of global metallogenetic patterns. *Ore Geol Rev* 89:946–987. <https://doi.org/10.1016/j.oregeorev.2016.03.014>
- Melezhik VA, Roberts D, Gorokhov IM, Fallick AE, Zwaan KB, Kuznetsov AB, Pokrovsky BG (2002) Isotopic evidence for a complex Neoproterozoic to Silurian rock assemblage in the north-central Norwegian Caledonides. *Precamb Res* 114:55–86
- Michallik RM, Wagner T, Fusswinkel T, Heinonen JS, Heikkilä P (2017) Chemical evolution and origin of the Luumäki gem beryl pegmatite: Constraints from mineral trace element chemistry and fractionation modeling. *Lithos* 274–275:147–168
- Mindat (2021) Slunkajavrre, Hamarøy, Nordland, Norway. <https://www.mindat.org/loc-247989.html>. Accessed 15 Jul 2021
- Müller A (2011) Potential of rare earth element and Zr-, Be-, U-, Th-, (W-) mineralisations in central and northern Nordland—Part 2. *Norges Geol Undersøkelse Rapport* 2011:021
- Müller A, Ihlen PM, Snook B, Larsen RB, Flem B, Bingen B, Williamson BJ (2015) The Chemistry of quartz in granitic pegmatites of southern Norway: Petrogenetic and economic implications. *Econ Geol* 110:1737–1757. <https://doi.org/10.2113/econgeo.110.7.1737>
- Müller A, Romer RL, Pedersen RB (2017) The Sveconorwegian pegmatite province—thousands of pegmatites without parental granites. *Can Mineral* 55:283–315
- Müller A, Simmons W, Beurlen H, Thomas R, Ihlen PM, Wise M, Roda-Robles E, Neiva AMR, Zagorsky V (2021) A proposed new mineralogical classification system for granitic pegmatites—Part I: history and the need for a new classification. *Can Mineral*. <https://doi.org/10.3749/canmin.1700088>
- Müller A, Snook B, Ihlen PM, Beurlen H, Breiter K (2013) Diversity of the quartz chemistry of NYF- and LCT-type pegmatites and its economic implications. Mineral deposit research for a high-tech world. In: *Proceedings of the 12th Biennial SGA Meeting*, Vol. 4, 12–15 August 2013, Uppsala, Sweden, ISBN 978-91-7403-207-9, pp 1774–1776
- Nordgulen Ø, Bickford ME, Nissen AL, Wortman GL (1993) U-Pb zircon ages from the Bindal Batholith, and the tectonic history of the Helgeland Nappe Complex, Scandinavian Caledonides. *J Geol Soc* 150(4):771–783
- Northrup CJ (1997) Timing structural assembly, metamorphism, and cooling of the Caledonian nappes in the Ofoten-Efjorden area, north Norway: tectonic insights from U-Pb and <sup>40</sup>Ar/<sup>39</sup>Ar geochronology. *J Geol* 105:565–582
- Osmundsen PT, Braathen A, Nordgulen Ø, Roberts D, Meyer GB, Eide E (2003) The Devonian Nesna shear zone and adjacent gneiss-cored culminations, North-Central Norwegian Caledonides. *J Geol Soc Lond* 60:1–14
- Rice AHN (2001) Field evidence for thrusting of the basement rocks coring tectonic windows in the Scandinavian Caledonides; an insight from the Kunes Nappe, Finnmark, Norway. *Nor Geol Tidsskr* 81:321–328
- Rice AHN, Anderson MW (2016) Restoration of the external Scandinavian Caledonides. *Geol Mag* 153:1136–1165. <https://doi.org/10.1017/S0016756816000340>
- Roberts D, Nordgulen Ø, Melezhik V (2007) The Uppermost Allochthon in the Scandinavian Caledonides: From a Laurentian ancestry through Taconian orogeny to Scandian crustal growth on Baltica. In: Hatcher RD Jr et al (eds) *4-D framework of continental crust*, Geological Society of America Memoir, vol 200, pp 357–377. [https://doi.org/10.1130/2007.1200\(18\)](https://doi.org/10.1130/2007.1200(18))
- Roberts D, Gee DG (1985) An introduction to the structure of the Scandinavian Caledonides. In: Gee DG, Sturt BA (eds) *The Caledonide Orogen—Scandinavia and related areas*. Wiley, New York, pp 55–68
- Roda-Robles E, Villaseca C, Pesquera A, Gil-Crespo PP, Vieira R, Lima A, Garate-Olave I (2018) Petrogenetic relationships between Variscan granitoids and Li-(F-P)-rich aplite-pegmatites in the Central Iberian Zone: Geological and geochemical constraints and implications for other regions from the European Variscides. *Ore Geol Rev* 95:408–430
- Romer RL (1997) U-Pb age of rare-mineral pegmatites at Stora Vika. *Geol Fören Stockh Förh* 119:291–294
- Romer RL (2003) Alpha-recoil in U-Pb geochronology: effective sample size matters. *Contr Mineral Petrol* 145:481–491
- Romer RL, Bax G (1992) The rhombohedral framework of the Scandinavian Caledonides and their foreland. *Geol Rundschau* 81(2):391–401
- Romer RL, Smeds S-A (1994) Implications of U-Pb ages of columbite-tantalites from granitic pegmatites for the Palaeoproterozoic accretion of 1.90–1.85 Ga magmatic arcs to the Baltic Shield. *Precambrian Res* 67:141–158
- Romer RL, Smeds S-A (1996) U-Pb columbite ages of pegmatites from Sveconorwegian terranes in southwestern Sweden. *Precambrian Res* 76:15–30
- Romer RL, Smeds S-A (1997) U-Pb columbite chronology of post-kinematic Palaeoproterozoic pegmatites in Sweden. *Precambrian Res* 82:85–99
- Romer RL, Wright JE (1992) U-Pb dating of columbitites: a geochronological tool to date magmatism, metamorphism, and ore deposits. *Geochim Cosmochim Acta* 56:2137–2142
- Romer RL, Kjøsnes B, Korneliussen A, Lindahl I, Skyseth T, Stendal M, Sundvoll B (1992) The Archaean-Proterozoic boundary beneath the Caledonides of northern Norway and Sweden:



- U-Pb, Rb-Sr and Nd isotope data from the Rombak-Tysfjord area. *Norges Geol Undersøkelse Report* 91:225
- Romer RL, Bax G, Kathol B (1994) Basement control of the Caledonian orogen along the Torneträsk section, northern Sweden. *Schweiz Mineral Petrogr Mitt* 74:469–481
- Romer RL, Nowaczyk N, Wirth R (2007) Secondary Fe-Mn-oxides in minerals heavily damaged by a-recoil: possible implications for palaeomagnetism. *Int J Earth Sci* 96:375–387
- Rudnick RL, Gao S (2004) Composition of the continental crust. In: Holland HD, Turekian KK (eds) *Treatise on geochemistry*, vol 3. Elsevier, Amsterdam, pp 1–64
- Schmitz MD, Schoene B (2007) Derivation of isotope ratios, errors and error correlations for U-Pb geochronology using  $^{205}\text{Pb}$ – $^{235}\text{U}$ –( $^{233}\text{U}$ )-spiked isotope dilution thermal ionization mass spectrometric data. *Geochim Geophys Geosyst* 8:Q08006
- Schuster R, Ilickovic T, Mali H, Huet B, Schedl A (2017) Permian pegmatites and spodumene pegmatites in the Alps: Formation during regional scale high temperature/low pressure metamorphism. In: Müller A, Rosing-Schow N (eds) *8th international symposium on granitic pegmatites. NGF abstracts and proceedings*, Kristiansand, Norway, pp 122–125
- Simmons WB, Lee MT, Brewster RH (1987) Geochemistry and evolution of the South Platte granite-pegmatite system, Jefferson County, Colorado. *Geochim Cosmochim Acta* 51:455–471
- Simmons WB, Falster A, Webber K, Roda-Robles E, Boudreaux AP, Grassi LR, Freeman G (2016) Bulk composition of Mt. Mica pegmatite, Maine, USA: implications for the origin of an LCT type pegmatite by anatexis. *Can Mineral* 54:1053–1070
- Simmons WB, Foord EE, Falster AU (1996) Anatectic origin of granitic pegmatites, Western Maine, USA, GAC-MAC Annual meeting—Abstracts with Programs, University of Manitoba, Winnipeg, USA
- Skår Ø (2002) U-Pb geochronology and geochemistry of early Proterozoic rocks of the tectonic basement windows in central Nordland, Caledonides of northcentral Norway. *Precambrian Res* 116:265–283
- Stacey JS, Kramers JD (1975) Approximation of terrestrial lead isotope evolution by a two-stage model. *Earth Planet Sci Lett* 26:207–221
- Steltenpohl MG, Andresen A, Tull JF (1990) Lithostratigraphic correlation of the Salangen (Ofoten) and Balsfjord (Troms) Groups: evidence for the postFinnmarkian unconformity, north Norwegian Caledonides. *Nor Geol Unders* 418:61–77
- Steltenpohl MG, Andresen A, Lindstrøm M, Gromet P, Steltenpohl LW (2003) The role of felsic and mafic igneous rocks in deciphering the evolution of thrust-stacked terranes: an example from the north Norwegian Caledonides. *Am J Sci* 303:149–185
- Steltenpohl MG, Andresen A (1991) Nappe sequences in the Ofoten region: Implications for terrane accretion, ophiolite obduction, and polyorogenic evolution. In: Andresen A, Steltenpohl MG (eds) *A geotraverse excursion through the Scandinavian Caledonides: Tornetrask-Ofoten-Troms: International Geologic Correlation Project*, vol 233, pp 4.1–4.19
- Steltenpohl MG, Bartley JM (1987) Thermobarometric profile through the Caledonian nappe stack of western Ofoten, north Norway. *Contrib Mineral Petrol*, vol 96, pp 93–103
- Stephens MB (1988) The Scandinavian Caledonides: a complexity of collisions. *Geol Today* 4:20–26
- Suominen V (1991) The chronostratigraphy of SW Finland with special reference to the Postjotnian and Subjotnian diabases. *Geol Surv Finland Bull* 1991:356
- Thelander T, Bakker E, Nicholson R (1980) Basement-cover relationships in the Nasafjäll Window, central Swedish Caledonides. *Geol Fören Stockh Förh* 102:569–580
- Thomas R, Davidson P (2016) Origin of miarolitic pegmatites in the Königshain granite/Lusatia. *Lithos* 260:225–241
- Tull JF, Bartley JM, Hodges KV, Andresen A, Steltenpohl MG, White JM (1985) The Caledonides in the Ofoten region (68°–69°N), north Norway: key aspects of tectonic evolution. In: Gee DG, Sturt BA (eds) *The Caledonide Orogen—Scandinavia and Related Areas*. Wiley, Chichester, pp 553–568
- Turekian KK, Wedepohl KH (1961) Distribution of the elements in some major unites of the Earth's crust. *Bull Geol Soc Am* 72:172–202
- Vaasjoki M, Rämö OT, Sakko M (1991) New U-Pb ages from the Wiborg rapakivi area: constraints on the temporal evolution of the rapakivi granite-anorthosite-diabase dike association of southeastern Finland. In: Haapala I, Condie KC (eds) *Precambrian granitoids—petrogenesis, geochemistry and metallogeny*. *Precambrian res*, vol 51, pp 227–243
- Villa IM, De Bièvre P, Holden NE, Renne PR (2015) IUPAC–IUGS recommendation on the half-life of  $^{87}\text{Rb}$ . *Geochim Cosmochim Acta* 164:382–385
- Webber K, Simmons WB, Falster AU, Hanson SL (2019) Anatectic pegmatites of the Oxford County pegmatite field, Maine, USA. In: Wise M, Brown C, Simmons WB, Roda-Robles E, Webber K (eds) *9th international symposium on granitic pegmatites*, Pala, California, USA, pp 87–90
- Wiest JD, Jacobs J, Fossen H, Ganerød M, Osmundsen PT (2020) Segmentation of the Caledonian orogenic infrastructure and exhumation of the Western Gneiss Region during transtensional collapse. *J Geol Soc Lond* 178:199. <https://doi.org/10.1144/jgs2020-199>
- Yoshinobu AS, Barnes CG, Nordgulen Ø, Prestvik T, Fanning M, Pedersen RB (2002) Ordovician magmatism, deformation, and exhumation in the Caledonides of central Norway: an orphan of the Taconic orogeny? *Geology* 30(10):883–886